Doctoral Thesis

Maintaining nuclear membrane homeostasis via degradation of the inner nuclear membrane protein Bqt4 by a ubiquitin-proteasome pathway

(核膜恒常性維持における核膜内膜タンパク質Bqt4の
ユビキチン-プロテアソーム依存的分解の意義)

Toan Khanh LE

Graduate School of Frontier Biosciences

Osaka University

March 2023

Abstract

Inner nuclear membrane (INM) proteins play important roles in maintaining the structural integrity and function of the nuclear envelope, the double membrane surrounding the nucleus. Aberrant accumulation of INM proteins has been linked to deformed nuclear morphology and certain diseases in mammals. However, the mechanisms by which INM homeostasis is maintained remain poorly understood. In this study, I used the fission yeast *Schizosaccharomyces pombe* to investigate the degradation mechanisms of the INM protein Bqt4. Previous work in our laboratory has shown that Bqt4 interacts with the transmembrane protein Bqt3 at the INM and is degraded in the absence of Bqt3. In this study, I found that excess Bqt4 that is not associated with Bqt3 is targeted for degradation by the ubiquitin-proteasome system localized in the nucleus, and that Bqt3 antagonizes this process. The degradation process involves the Doa10 E3 ligase complex at the INM. In addition, I proved that Bqt4 is a tail-anchored protein and extraction from the membrane by the Cdc48 complex is required for its degradation. I also found that the C-terminal transmembrane domain of Bqt4 is necessary and sufficient for proteasome-dependent protein degradation. Remarkably, accumulation of excess Bqt4 at the INM impaired cell viability and caused nuclear envelope deformation, suggesting that proper control of Bqt4 levels is important for maintaining nuclear membrane homeostasis. These findings provide new insights into the mechanisms that regulate INM protein homeostasis and may have implications for understanding the role of INM proteins in diseases.

Table of Contents

Chapter 1 Introduction

1-1 The inner nuclear membrane proteins

The nucleus is the central structure within eukaryotic cells that contains the genetic material. It is enclosed by the nuclear envelope (NE), a double membrane that separates the nucleoplasm from the cytoplasm. The NE comprises the inner nuclear membrane (INM) and the outer nuclear membrane (ONM). While the ONM is connected with the endoplasmic reticulum (ER) and contains proteins common with the ER, the INM is separated from the ONM by nuclear pore complexes (NPCs) and houses a distinct set of proteins that interact primarily with the nucleoplasm.

Proteins associated with the INM are involved in many fundamental processes that are essential for the proper functioning of the nucleus. These INM proteins have been shown to play critical roles in a diversity of nuclear processes, including chromatin organization, control of gene expression, DNA replication and repair, genome stability, and maintenance of nuclear structure (Mekhail and Moazed, 2010; Hirano et al., 2020a; Pawar and Kutay, 2021). Dysregulation of INM proteins has been linked to various diseases, highlighting the importance of understanding the mechanisms that regulate INM homeostasis (Janin et al., 2017).

There are several well-characterized INM proteins in mammalian cells. One of the first INM proteins to be identified is lamin B receptor (LBR) (Worman et al., 1988). It has been suggested that LBR plays a role in the attachment of chromatin to the NE and the formation of heterochromatin (a type of densely packed and transcriptionally inactive chromatin) underneath the NE in mammalian cells (Hirano et al., 2012; Solovei et al., 2013).

Another well-studied family of INM proteins is the LEM (LAP2-Emerin-MAN1)-domain proteins, a group of proteins that includes LAP2 (lamin A-interacting protein 2),

emerin, and MAN1. In addition to these three proteins, LEM2, several splice variants of LAP2 and others are also classified as LEM domain proteins. These proteins are involved in a variety of cellular processes, including NE assembly, cell cycle control, chromatin organization, and heterochromatin formation. Lem2 is particularly notable among the LEM domain proteins due to its high degree of conservation across species from yeasts to humans, indicating that it may have a conserved role in chromosomes (Hirano et al., 2020a).

The SUN (Sad1p, Unc-84)-domain proteins, another group of INM proteins that includes SUN1 and SUN2 in mammals, form the LINC (LInker of Nucleoskeleton and Cytoskeleton) complex by linking up with the KASH (Klarsicht, ANC-1, Syne-1 homology)-domain proteins such as nesprins in the ONM. SUN proteins also attach to lamins in the nuclear lamina, and some KASH proteins link to cytoskeletal proteins such as actin, enabling communication between the cytoskeleton and the nucleoskeleton (Pawar and Kutay, 2021). Besides these proteins, there are hundreds of other candidates for INM protein in mammalian cells that have yet to be characterized and their significance remains unexplored (Hirano et al., 2020a; Pawar and Kutay, 2021).

Underneath the INM lies the nuclear lamina, a protein meshwork composed principally of lamins, which are intermediate filament-like proteins, and lamin-associated proteins. In addition to providing structural support to the NE, the nuclear lamina plays significant roles in chromosome structure and function through its interaction with heterochromatin regions known as lamina-associated domains (LADs). It should be noted that the nuclear lamina is exclusive to animal cells, and is absent in other eukaryotic species such as yeasts and plants (Hirano et al., 2020a).

Since the INM is continuous with the ER, its unique composition must be achieved by special targeting mechanisms. INM proteins are generally synthesized in the ER and inserted into its membrane. Subsequently, they are transported into the INM by passive diffusion

provided that the molecular size is sufficiently small and retained there via interactions with nuclear components, such as chromatin. Alternatively, INM proteins can be actively transported from the ER into the nucleus by the NPC, a process requiring a nuclear localization signal (NLS) and an intrinsically disordered sequence (Katta et al., 2014).

Excess amounts of INM proteins cause aberrant accumulation at the NE, often causing nuclear deformation and malfunctioning (Gonzalez et al., 2012). The aberrant accumulation of INM proteins has been linked to certain mammalian diseases. For example, accumulation of the INM protein SUN1 was found to be pathogenic in human laminopathies, such as Emery-Dreifuss muscular dystrophy and Hutchinson-Gilford progeria syndrome (Chen et al., 2012). Therefore, the amounts of INM proteins must be regulated. However, the mechanisms that regulate levels of resident INM proteins to maintain INM homeostasis remain poorly understood.

1-2 The INM protein Bqt4 in the fission yeast *S. pombe*

The study of INM proteins in the model organism *Schizosaccharomyces pombe*, also known as fission yeast, has the potential to provide insights into the mechanisms underlying the maintenance of nuclear membrane homeostasis in eukaryotes. Fission yeast *S. pombe* has several advantages as a model system for this research, including its relatively small number of INM proteins and the ease of genetic analysis.

In *S. pombe*, several INM proteins have been studied for their roles in the organization and regulation of the chromosomes, including Ima1, Lem2, Man1, and Bqt4 (Figures 1-1, 1-2) (Chikashige et al., 2006; Chikashige et al., 2009; Hiraoka et al., 2011; Steglich et al., 2012; Gonzalez et al., 2012; Tange et al., 2016; Hirano et al., 2020b). Among them, our lab found that Bqt4 is required for anchoring telomeres to the NE during vegetative growth through the telomere-associated protein complex Taz1-Rap1 (Figure 1-2) and for

clustering telomeres to the spindle-pole body through the meiosis-specific telomere-binding proteins, Bqt1 and Bqt2 (Chikashige et al., 2006; Chikashige et al., 2009). Bqt4 also directly binds to DNA, facilitating telomere tethering to the NE (Figure 1-2) (Hu et al., 2019). In addition, Bqt4 interacts with Lem2 and is required for localization of Lem2 in the INM regions outside of the centromere core (Figure 1-2) (Hirano et al., 2018; Ebrahimi et al., 2018). Importantly, Bqt4 shares redundant functions, independent of telomere anchoring, with Lem2, and the depletion of Bqt4 is synthetic-lethal with the depletion of Lem2 (Figure 1-2) (Tange et al., 2016; Kinuagsa et al., 2019). Therefore, it is expected that Bqt4 plays important roles in cell viability. Structurally, Bqt4 is predicted to be a tail-anchored protein (Figure 1-3). Additionally, Bqt4 interacts with Bqt3, which is predicted to be a seven-pass transmembrane protein, and helps recruiting Bqt3 to the INM (Figure 1-3) (Chikashige et al., 2009). Interestingly, Bqt4 is degraded in the absence of Bqt3, suggesting that Bqt3 protects Bqt4 from degradation (Chikashige et al., 2009). However, the non-telomeric vital roles of Bqt4 and the mechanisms underlying its degradation remain unknown.

1-3 Protein degradation and the ubiquitin-proteasome system

Eukaryotic cells regulate the levels of proteins by controlling not only rates of their synthesis, but also rates of their degradation. Therefore, protein degradation is essential for maintaining the balance of intracellular components. In addition, protein degradation plays a central role in various fundamental cellular processes, including regulation of signaling pathways, cell cycle control, and protein quality control. For example, rapidly degraded proteins can serve as regulatory molecules in signaling pathways, as their rapid turnover allows them to respond quickly to stimuli. Protein degradation is also important for protein quality control that is the process by which damaged, misfolded or mislocalized proteins are recognized and eliminated.

There are two principal pathways mediating protein degradation in eukaryotic cells: the ubiquitin-proteasome system (UPS) and the lysosome-autophagy system (Ciechanover, 2005). The UPS involves the covalent attachment of small proteins called ubiquitins to target proteins, marking them for degradation by the proteasome, which is a large, multisubunit protease complex found in the cytosol and nucleus of cells. The lysosome-autophagy system involves the degradation of proteins within specialized organelles called lysosomes through autophagy that is a process by which cells engulf and degrade unnecessary or dysfunctional cellular components, including proteins.

The UPS is the primary mechanism responsible for selective degradation of the majority of proteins in the nucleus, cytosol, ER and mitochondria of eukaryotic cells. In the UPS, the substrate protein is conjugated with a polyubiquitin chain, leading to its subsequent recognition and degradation by the 26S proteasome. First, a ubiquitin molecule is covalently attached to the amino group of the side chain of a lysine residue on the target protein. Then, the ubiquitin itself is ubiquitinated at one of its lysine residues. This process continues, resulting in the formation of a polyubiquitin chain. The polyubiquitinated protein is finally recognized and cleaved by the proteasome complex. Ubiquitination is a process involving a cascade of three different enzymes: ubiquitin-activating enzymes (E1s), ubiquitin-conjugating enzymes (E2s), and ubiquitin ligases (E3s). In brief, E1s activate ubiquitin and transfer it to E2s, which in turn transfer it to the target protein through the action of E3s (Hochstrasser, 1996; Hershko and Ciechanover, 1998; Varshavsky, 2012).

1-3-1 The proteasome

Protein degradation by the UPS is carried out by the 26S proteasome, a large and highly organized protein complex that degrades proteins marked for destruction by ubiquitin. The 26S proteasome is found in all eukaryotes, being highly conserved across different species. It

is composed of two main assemblies: the 20S core particle (CP), which contains protease active sites, and the 19S regulatory particle (RP), which recognizes and binds to proteins targeted for degradation. Together, the CP and the RP work to degrade proteins in a highly selective and efficient manner. Proteins targeted for degradation are first recognized and bound by the RP, and then translocated into the CP, where they are cleaved into small peptides. The resulting peptides are then released from the proteasome and can be further degraded by other cellular enzymes.

The CP is a barrel-shaped structure that is composed of four stacked rings, two outer rings and two inner rings, also known as α and β rings, respectively. Each ring is made up of seven distinct subunits. Only the inner β rings contain subunits with proteolytic active sites (β1, β2, and β5), which are located within the interior cavity of the CP. The outer α rings help to control access to the active sites in the internal space of the CP and prevent nonspecific proteolysis. The substrate is transported to the CP through a narrow substrate translocation channel, which can be in either a closed or open state (Finley, 2009; Finley et al., 2012).

The RP, which is located at one end of the CP, consists of two subcomplexes: the base, which is made up of ten different subunits, and the lid, which is made up of nine subunits. The RP is involved in multiple functions, including recognizing and binding to ubiquitinated substrates, directing substrates into the substrate translocation channel, unfolding them before they are transported into the channel, removing the polyubiquitin tag and regulating the proteasome activity. In particular, substrate unfolding and translocation are actively facilitated by six ATPases, known as Rpt1-Rpt6, which make up a heterohexomeric ring complex in the RP base (Finley, 2009; Finley et al., 2012).

1-3-2 Ubiquitin and ubiquitination

Ubiquitin is a small, highly conserved protein that is ubiquitously expressed in all eukaryotic cells. Composed of 76 amino acids, ubiquitin has a molecular weight of approximately 8.6 kDa. Its major function is to serve as a signal that targets proteins for proteasome-mediated degradation. This is accomplished via the process of ubiquitination, in which a polyubiquitin chain is covalently attached to lysine residues on the target protein (Pickart and Eddins, 2004).

Ubiquitination is a highly regulated, multistep process involving the sequential action of three enzymes. In the first step, the ubiquitin molecule is activated by being attached to an E1 ubiquitin-activating enzyme. The activated ubiquitin is then transferred to an E2 ubiquitin-conjugating enzyme, which can transfer the ubiquitin to a lysine residue of the target protein or another ubiquitin, forming a polyubiquitin chain. This process also requires a third component called E3 ubiquitin ligase, which generally forms a complex with E2 enzyme and directly binds to the target protein, facilitating the transfer of ubiquitin from the E2 to the substrate. In some cases, the ubiquitin may be transferred from E2 to E3 and then from E3 to the substrate. The E3 acts as a substrate receptor and is responsible for substrate specificity, recognizing specific degradation signals, also known as “degrons”, on the the target protein (Pickart, 2001; Varshavsky, 2012).

Since E3 ubiquitin ligases are the primary determinants of the specificity of the UPS, most cells have a small number of E1 and E2 enzymes but a much larger number of E3 ligases. The human cell is predicted to possess 2 E1 enzymes (Groettrup et al., 2008), around 40 E2 enzymes (Stewart et al., 2016), and 500-1000 E3 enzymes (Nakayama and Nakayama, 2006). Likewise, the budding yeast cell contains 1 E1, 11 E2, and 60-100 E3 enzymes (Finley et al., 2012).

There are two major classes of E3 ligases: RING-finger (Really Interesting New Gene), and HECT (Homologous to the E6-AP Carboxyl Terminus). In humans, there are only 28 HECT E3 ligases, while the vast majority (~95%) are members of the RING-finger family. Similarly, budding yeast has only 5 HECT E3 ligases, with the majority of 65 belonging to the RING-finger family. While HECT E3s can receive the ubiquitin from the E2 enzyme by forming a thioester bond with the ubiquitin before transferring it to the substrate (Rotin and Kumar, 2009), RING-finger E3s act as scaffolds that bring the E2 enzyme in close proximity to the substrate in order to facilitate the direct transfer of ubiquitin (Deshaies and Joazeiro, 2009). In addition to RING-finger and HECT E3s, two other minor types known as U-box and PHD-finger (Plant Homeo Domain) have also been defined (Nakayama and Nakayama, 2006).

1-4 Degradation pathways in the ER and INM

1-4-1 ER-associated degradation

Mechanisms for ER membrane homeostasis have been well studied: ER membrane proteins are regulated through the ER-associated degradation (ERAD) system, which is involved in degrading misfolded or mislocalized ER proteins (Vembar and Brodsky, 2008; Ruggiano et al., 2014; Christianson and Carvalho, 2022). It has been shown that in the budding yeast *Saccharomyces cerevisiae*, ERAD involves the UPS, and ER-localized E3 ubiquitin ligases such as Hrd1 and Doa10 (human MARCHF6/TEB4).

ERAD requires additional machinery for the degradation of integral membrane proteins, involving Cdc48/p97, an ATPase associated with diverse cellular activities (AAA-ATPase), which removes the ubiquitinated proteins from the membrane before transferring them to the proteasome for degradation (Ruggiano et al., 2014; Christianson and Carvalho, 2022; Koch and Yu, 2019; Smoyer and Jaspersen, 2019; Mannino and Lusk, 2022).

1-4-2 INM-associated degradation

INM-associated degradation (INMAD), which also depends on the UPS, has been proposed as an extension of ERAD to maintain INM homeostasis (Foresti et al., 2014; Khmelinskii et al., 2014; Koch and Yu, 2019; Smoyer and Jaspersen, 2019; Mannino and Lusk, 2022). In budding yeast, INMAD has been found to be mediated primarily by membrane E3 ligases such as Doa10 and the Asi complex. The Doa10 complex can passively diffuse from the ER to the INM and is known to ubiquitinate mainly soluble nuclear substrates such as the transcription factor MATα2 (Deng et al., 2006; Ravid et al., 2006). The Asi complex is an INM resident which is primarily involved in degrading mislocalized or unassembled ER proteins as a means of quality control (Foresti et al., 2014; Khmelinskii et al., 2014; Natarajan et al., 2020).

Noticeably, only a few of the characterized INMAD substrates were resident INM proteins. Reported INM protein substrates include Asi2, which is a subunit of the Asi complex and is a substrate of Doa10 (Boban et al., 2014), Pom33, which is ubiquitinated by the Asi compex to regulate its distribution instead of affecting protein turnover (Smoyer et al., 2019), and Msp3, which is a substrate of the soluble APC/C complex (Koch et al., 2019). Moreover, structural or functional homologs of the Asi proteins are absent in other species. Importantly, it is still not clear whether INMAD mechanism operates in a similar manner in other species, despite the fact that there is growing evidence that degradation of INM proteins in mammals also employs the UPS (Tsai et al., 2016; Khanna et al., 2018; Khrshnan et al., 2022). Therefore, our understanding of INM protein degradation is far from adequate.

1-5 The aim of the thesis

In this study, I aimed to:

1) Identify the molecular factors essential for degradation of the INM protein Bqt4 in *S. pombe*. By elucidating the mechanisms by which Bqt4 is degraded, my objective was to obtain a better understanding of the processes that govern protein degradation at the INM.
2) Investigate the potential biological significance of Bqt4 degradation to gain insights into the biological significance of INM protein degradation and the roles of INM proteins in diseases.

Chapter 2 Materials and methods

2-1 Yeast strains and culture media

All *S. pombe* strains used in this study are listed in Table S1. Unless otherwise specified, all *S. pombe* strains were cultured in yeast extract with supplements (YES) medium. Malt extract medium (ME) was used to induce sporulation. G418 disulfate (Nacalai Tesque, Japan), Hygromycin B (Wako, Japan), nourseothricin sulfate (Werner BioAgents, Germany), and Blasticidin S (Wako, Japan) were used at concentrations of 100, 200, 100, and 100 μg/ml, respectively, to select strains bearing the respective selection marker.

2-2 Construction of plasmids and strains

All plasmids were constructed using the NEBuilder system (New England BioLabs, MA, USA) and enzymatic digestion and ligation (TaKaRa, Japan) systems, according to the manufacturer's instructions. Gene disruption and GFP tagging were performed using the direct chromosomal integration method (Wach, 1996; Bähler et al., 1998). The integration cassettes were amplified using a two-step PCR. In the first PCR, fragments (~500 bp genomic regions upstream and downstream of the gene of interest) were amplified from the wild-type *S. pombe* genome using the KOD One DNA polymerase (TaKaRa Bio Inc., Japan). The first PCR products were used as primers in the second step of the PCR to amplify a cassette for integration, which contained a selection marker. For gene disruption, pFA6-kanMX6 (Bähler et al., 1998), pCR2.1-hph, pCR2.1-bsd, and pCR2.1-nat (Sato et al., 2005) were used to generate the integration cassettes. For GFP tagging, pFA6-GFP(S65T)-kanMX6 (Bähler et al., 1998) was used to generate the GFP-containing integration cassettes. The cassettes were then transformed into *S. pombe* cells and the desired integrant strains were selected on YES plates containing the appropriate selection agent. Correct disruptions and

integrations were confirmed by genomic PCR at the 5′ and 3′ ends using KOD FX Neo (TaKaRa Bio Inc., Japan).

2-3 Fluorescence microscopy

Fluorescence microscopy data of intracellular GFP fusion proteins in living cells were collected using a DeltaVision microscope system (GE Healthcare Inc., USA) equipped with a pco.edge 4.2 sCMOS camera (PCO, Germany) and a ×60 PlanApo N OSC oil-immersion objective lens (numerical aperture NA=1.4, Olympus, Japan). For live-cell imaging, cells were precultured from a fresh colony, followed by culturing in YES medium at 30°C to reach the logarithmic growth phase (5-10×10^6 cells/ml). The cells were then attached to glass-bottomed culture dishes coated with soybean lectin (Sigma-Aldrich, USA), covered with Edinburgh minimal medium with glutamate (EMMG) medium, and observed at specified temperatures.

2-4 Image quantification and processing

An identical fluorescence intensity range was applied to all images in each panel using the Fiji software (Schindelin et al., 2012).

To quantify the fluorescence intensity in the nucleus, I used Fiji software. First, I generated the sum projection image from the raw z-stack images and then subtracted the background signal from the entire image by measuring the mean intensity of a region where no cells exist. Second, the nuclear region was manually or semi-automatically selected. For semi-automatic selection, individual nuclei were selected (original image), and the selected image was blurred using Gaussian blur (blurred image). An appropriate sigma value was applied depending on the image contrast. By subtracting the blurred image from the original image, an edge-enhanced image was generated. The nuclear region was thresholded using the

appropriate minimum and maximum intensity ranges. Third, the threshold region was applied to the original image and the total fluorescence intensity of the region was quantified. The nuclear intensities obtained from *bqt3*$^{+}$ cells were averaged and the values were used to calculate the relative fluorescence intensity. The relative fluorescence intensities were plotted, and the results are presented as the mean ± standard deviation.

For the roundness index measurement, after selecting individual nuclei, the nuclear membrane signal was thresholded using the appropriate fluorescence intensity ranges. The nuclear region was filled in, and the roundness index was measured using the built-in function in Fiji.

2-5 Western blotting

Cells were precultured in YES medium at 30°C overnight, inoculated in fresh YES, and then cultured until the cell concentration reached the mid-log phase (5-10×10^6 cells/ml). Approximately 5×10^7 cells were harvested by centrifugation at 4°C, and the cell pellet was washed with 1 ml ice-cold water containing 1 mM phenylmethylsulfonyl fluoride (PMSF). Cells were lysed in 150 µl of ice-cold 1.85 M NaOH containing 7.5% β-mercaptoethanol (β-ME) on ice for 15 min, followed by the addition of 150 µl of ice-cold 55% (v/v) trichloroacetic acid (TCA) to precipitate the proteins, incubation on ice for 15 min, and centrifugation (10 min, 14,000 ×g, 4°C). The protein pellet was then washed twice with ice-cold acetone and dissolved in sample solubilization buffer [50 mM Tris-HCl pH 8.0, 1% SDS, 1× Protease Inhibitor Cocktail (P8215, Sigma-Aldrich, USA), 1 mM PMSF, 1 mM bortezomib]. Total protein concentrations were determined using the BCA assay (Thermo Fisher Scientific, USA) according to the manufacturer's protocol. The samples were further diluted in 2× Laemmli SDS sample buffer to a concentration of 1 µg/µl. After the addition of dithiothreitol to a concentration of 50 mM, samples were heated at 95°C for 10 min before

immunoblotting. Identical amounts of protein (10 μg) were separated by SDS–PAGE and transferred to a polyvinylidene difluoride membrane. The membranes were blocked for 1 h at room temperature (approximately 26-28°C) in blocking solution PBST (10 mM Na_2HPO_4, 137 mM NaCl, 2.7 mM KCl, 1.76 mM KH_2PO_4, and 0.1% Tween 20) containing 5% skim milk (Nacalai Tesque, Japan). To detect the GFP fusion proteins and β-actin as a loading control, the membranes were probed with anti-GFP rabbit polyclonal antibody (Rockland, USA; 1:2,000 dilution) or anti-β-actin mouse monoclonal antibody (Abcam, UK; 1:2,000 dilution) in blocking solution overnight at 4°C. After three rounds of washing with PBST, the membranes were incubated with the appropriate horseradish peroxidase-conjugated secondary antibodies (1:2,000 dilution, Cytiva, USA) in a blocking solution at room temperature for 2 h. After three rounds of washing with PBST, immunoreactive bands were detected using a chemiluminescence system (ImmunoStar LD, Wako, Japan) in a ChemiDoc imaging system (Bio-Rad, USA).

2-6 Proteasome inhibition

Cells were grown in YES medium to the early mid-log phase (2-5×10^6 cells/ml), as described above. The culture was then divided into two, and the proteasome inhibitor bortezomib (LC Laboratories, USA) dissolved in dimethyl sulfoxide (DMSO) was added to one culture to a final concentration of 1 mM, and the same amount of DMSO was added to the other culture. Cells were incubated at 26°C for 4 h before harvesting for fluorescence microscopy or immunoblotting.

2-7 Temperature sensitive mutant experiments

For the temperature-sensitive mutant experiments, cells harboring *ts* or *cs* mutations were grown in YES medium to the early mid-log phase (2-5×10^6 cells/ml) at 26°C and 33°C,

respectively. The culture temperature was shifted up to 36°C or down to 16°C, and then the cells were incubated for 4 h and 15 h before harvesting, respectively.

2-8 Ubiquitination detection assay

The ubiquitination detection assay was performed as described previously (Boban et al., 2014) with modifications. Cells were grown in YES medium at 30°C until the mid-log phase (5-10×10^6 cells/ml), and approximately 5×10^8 cells were harvested by centrifugation at 4°C. Where indicated, the proteasome inhibitor bortezomib was added to a final concentration of 1 mM for 4 h before the cells were collected. The same volume of DMSO was added to the control samples. The cells were washed with cold water containing 1 mM PMSF and lysed in 250 µl of 1.85 N NaOH solution containing 7.5% β-ME for 15 min on ice. Subsequently, the proteins were precipitated by adding 250 µl of 55% (v/v) TCA, followed by incubation for 15 min on ice. The proteins were pelleted by centrifugation (10 min, 14,000 ×g, 4°C) and washed with 500 µl of 50 mM Tris before being dissolved in 200 µl denaturation solution [25 mM Tris-HCl pH 7.4, 2% SDS, 2 mM ethylenediaminetetraacetic acid (EDTA), 1× Protease Inhibitor Cocktail (P8215, Sigma-Aldrich, USA), 1 mM PMSF, 1 mM bortezomib, 10 µM PR-619 (SML0430, Sigma-Aldrich, USA), and 50 mM 2-chloroacetamide (032-09762, Fuji film Wako, Japan)]. Total protein concentrations were determined using the BCA assay (Thermo Fisher Scientific, USA) according to the manufacturer's protocol. The samples were incubated at 65°C for 10 min and clarified by centrifugation (5 min, 15,000 ×g, room temperature). Equal amounts of protein lysates were diluted five-fold with cold IP dilution buffer (50 mM Tris-HCl pH 7.5, 1.2% Triton X-100, 2 mM EDTA, 100 mM NaCl, 1 × Protease Inhibitor Cocktail (P8215, Sigma-Aldrich, USA), 1 mM PMSF, 1 mM bortezomib, 10 µM PR-619, and 50 mM 2-chloroacetamide), incubated with gentle rotation at 4°C for 1 h, and cleared by centrifugation at 14,000 ×g for 10 min. A portion (20 µl) of the sample (2%

input) was combined with 2× Laemmli SDS sample buffer (20 µl) and frozen until analysis. The remaining sample was mixed with antibody-coupled beads prepared from 2 µg anti-GFP rabbit polyclonal antibody (Rockland) and 50 µl Protein-A-coupled Dynabeads (Life Technologies, USA) according to the manufacturer's instructions. The samples were immunoprecipitated at 4°C for 3 h with gentle rotation and pelleted using a magnet. The pellets were then washed as follows: twice with washing solution A (50 mM Tris-HCl pH 7.4, 2 mM EDTA, 100 mM NaCl, 1% Triton X-100, 0.4% SDS), once with washing solution B (50 mM Tris-HCl pH 7.4, 2 mM EDTA, 350 mM NaCl, 1% Triton X-100) including a 10-min incubation at 4°C with gentle rotation, and finally once with washing solution A. To elute the immunoprecipitated protein, 50 µl of 1× Laemmli SDS sample buffer was added to the pellet, and the mixture was incubated for 10 min at 65°C. Ten microliters of each sample were separated on SDS-PAGE gels (8%). For the analysis of immunoprecipitated GFP-Bqt4, the eluate was diluted 1:20 with 1× Laemmli SDS sample buffer. Immunoblotting analysis was performed using an anti-GFP mouse monoclonal antibody (JL8; 1:1000; TaKaRa Bio Inc., Japan) and an anti-ubiquitin mouse monoclonal antibody (P4D1, 1:1000; Santa Cruz Biotechnology, USA). Protein levels in the input samples were assessed using an anti-β-actin antibody (1:2000; Abcam).

2-9 Membrane association assay

The membrane association assay was performed according to a previously published protocol (Habeck et al., 2015) with slight modifications. *S. pombe* cells expressing GFP-Bqt4 and control proteins (GFP-Bqt3 and GFP-ADEL) were grown to the mid-log phase and mixed at a 1:1:1 ratio before cell harvesting by centrifugation at 4°C. The harvested cells (~5×10^8 cells) were washed with cold water containing 1 mM PMSF and resuspended in 500 µl cold fractionation buffer (FB; 0.7 M sorbitol, 50 mM Tris-HCl pH 7.4, 1× Protease Inhibitor

Cocktail, 1mM PMSF, 1 mM bortezomib). Resuspended cells were lysed using a bead shocker (2,700 rpm for 10 cycles of 60 s on and 60 s off; Yasui Kikai, Co., Japan), followed by washing the beads three times with 200 µl FB. The cell extracts were combined and debris was removed by centrifugation (600 ×g for 5 min at 4°C). The lysate was divided into five separate aliquots that were subjected to one of the following treatments: (1) FB alone; (2) 0.1 M Na_2CO_3, pH 11; (3) 2.5 M urea; (4) 0.5 M NaCl; or (5) 1% Triton X-100 and 0.5 M NaCl. After incubation for 1 h on ice with occasional mixing, the samples were separated into pellet (P) and supernatant (S) fractions by ultracentrifugation at 50,000 ×g for 45 min at 4°C. The pellets were washed once with appropriate supplemented FB by centrifugation (50,000 ×g for 45 min at 4°C) before being resuspended in FB. Proteins were then precipitated from the pellet and supernatant fractions by adding 150 µl of 55% (v/v) TCA. After 15 min of incubation on ice, the proteins were pelleted by centrifugation (16,000 ×g for 10 min at 4°C), washed twice with ice-cold acetone, and dissolved in dye-free 2× Laemmli SDS sample buffer. Total protein concentrations were measured using the BCA assay, as described above. The samples were incubated for 10 min at 95°C before immunoblotting.

2-10 Spot assay

Cells expressing GFP-Bqt4 under the control (*bqt4p*) or nmt1 promoter (*nmt1p*) were precultured in YES medium overnight. Five-fold dilution series of the cells (starting concentration was 8.0×10^5 /mL) were spotted on the EMMG medium plates supplemented with or without 10 µM thiamine, and then the plates were incubated at 30°C for 4 days.

For the temperature-sensitivity growth assay, wild-type and Cdc48 mutant cells were spotted in a five-fold dilution series and incubated at 16, 20, 26, 30, 33 and 37°C for 3-6 days.

Chapter 3 Results

3-1 INM protein Bqt4 is degraded via the ubiquitin-proteasome system

Because the ubiquitin-proteasome system accounts for the selective degradation of many proteins in the nucleus (Enam et al., 2018; Franić et al., 2021), I first tested the requirement of the proteasome for Bqt4 degradation. I treated cells expressing N-terminally GFP-tagged Bqt4 (GFP-Bqt4) under its own promoter with bortezomib (BZ), a chemical proteasome inhibitor working in *S. pombe* (Takeda et al., 2011), and assessed the fluorescence levels of GFP-Bqt4 at 4 h after drug addition in the presence or absence of Bqt3. As a result of the treatment, GFP-Bqt4 fluorescence in the nuclei of both *bqt3*$^{+}$ and *bqt3Δ* cells was elevated (Figure 3-1A). To confirm this result, I checked protein levels by Western blotting, which consistently showed an increase in GFP-Bqt4 protein levels in these strains upon proteasomal inhibition by BZ (Figure 3-1B). Notably, the GFP-Bqt4 signal was not only restored upon proteasome inhibition in the absence of Bqt3, but also elevated even in the presence of Bqt3. This suggests that Bqt4 is constitutively turned over by the proteasome system and its association with Bqt3 antagonizes this process. I sought to confirm this phenomenon by introducing the temperature-sensitive *mts3-1* proteasome mutation (Gordon et al., 1996). Using both fluorescence microscopy and Western blotting, I found that GFP-Bqt4 levels increased in *bqt3*$^{+}$ and *bqt3Δ* cells carrying this proteasome mutation at the restrictive temperature of 36°C, as compared to the corresponding wild-type strains (Figure 3-1C, D). These results indicate that Bqt4 degradation proceeds via the proteasome system.

Since proteins are ubiquitinated as a requirement for recognition by the proteasome, I examined whether Bqt4 is modified by polyubiquitination. I immunoprecipitated GFP-Bqt4 under denaturing conditions and detected associated ubiquitin by immunoblotting. Ubiquitinated forms of Bqt4 were detected in *bqt3*Δ cells and were enriched in both *bqt3*$^{+}$

and *bqt3*Δ cells when proteasomal activity was inhibited (Figure 3-1E), suggesting that Bqt4 is targeted to the proteasome by polyubiquitin modification.

Vacuolar autophagy is another pathway through which cells degrade proteins. Thus, I next examined whether Bqt4 degradation is regulated by the vacuolar autophagy pathway by analyzing GFP-Bqt4 levels in *bqt3*Δ cells lacking *isp6* and *atg1* genes. Isp6 is a serine protease necessary for vacuolar function, and Atg1 is a serine/threonine protein kinase that is the upstream initiator of the autophagy machinery. Deletion of these two genes has been shown to completely impair the vacuolar autophagy pathway (Kohda et al., 2007). I found that the deletion of *isp6* and *atg1* had no detectable effect on the quantity of GFP-Bqt4 in the absence of Bqt3, suggesting that Bqt4 degradation does not involve the vacuolar autophagy system (Figure 3-1F). Collectively, I concluded that the Bqt4 protein is degraded by the ubiquitin-proteasome system, without involvement of the vacuolar autophagy pathway.

3-2 Bqt4 degradation occurs in the nucleus

Next, I attempted to determine whether Bqt4 was degraded in the nucleus by the nuclear proteasome. In *S. pombe*, proper targeting of proteasomes to the nucleus requires the tethering factor Cut8 (Figure 3-2A) (Tatebe and Yanagida, 2000; Takeda and Yanagida, 2005). In *cut8* mutants, proteasomes fail to localize in the nucleus and become mostly cytoplasmic (Tatebe and Yanagida, 2000). Because nuclear protein degradation depends on the localization of proteasomes in the nucleus (Tatebe and Yanagida, 2000; Takeda and Yanagida, 2005), I examined the level of GFP-Bqt4 in *bqt3*$^{+}$ and *bqt3Δ* cells carrying the temperature-sensitive *cut8-563* mutation. I found that GFP-Bqt4 degradation was suppressed in *cut8-563* cells shifted to the nonpermissive temperature of 36°C (Figure 3-2B, C). These results strongly suggest that Bqt4 is degraded mainly by the proteasome within the nucleus.

3-3 Bqt4 degradation involves the Doa10 E3 ligase complex

I next sought to identify the specific E3 ubiquitin ligase that directly recognizes Bqt4. As Bqt4 is a protein associated with the INM, I investigated whether membrane-localized Hrd1 and Doa10 E3 ligases participate in the Bqt4 degradation pathway. Deletion of *doa10*$^{+}$ partially restored GFP-Bqt4 levels in the absence of Bqt3, whereas deletion of *hrd1*$^{+}$ did not (Figure 3-3A, B, comparing *hrd1*Δ to *doa10*Δ). These results are consistent with previous studies that showed that Doa10 partially localizes to the INM and is involved in the degradation of certain nuclear and INM substrates, whereas Hrd1 is found exclusively in the ER (Deng and Hochstrasser, 2006; Boban et al., 2014). Additionally, the double deletion of *doa10*$^{+}$ and *hrd1*$^{+}$ showed no obvious synthetic effect on GFP-Bqt4 restoration compared to the deletion of *doa10*$^{+}$ alone (Figure 3-3A, B). I also checked the quantity of GFP-Bqt4 in mutants lacking Ubc6 and Ubc7, which are E2 ubiquitin-conjugating enzymes associated with Doa10 (Swanson et al., 2001). I found that GFP-Bqt4 levels increased to some extent in *ubc6*Δ, *ubc7*Δ single, and *ubc6*Δ *ubc7*Δ double mutants (Figure 3-3C, D). These findings indicate that the Doa10 complex contributes to the degradation of Bqt4 in the INM.

Although degradation of Bqt4 depended on Doa10, the level of GFP-Bqt4 was only partially restored in the *doa10*Δ mutant (Figure 3-3A, B). Therefore, I attempted to search for other redundant E3 ligases involved in Bqt4 degradation. I constructed mutants of E3 ligases and their components that are suggested to localize or function in the ER and nucleus, namely *meu34*Δ, *dsc1*Δ, *ubr1*Δ, *ubr11*Δ, *san1*Δ, *hul5*Δ, *ptr1-1*, and *cut9-665* (PomBase, Matsuyama et al., 2006, Nielsen et al., 2014; Enam et al., 2018; Franić et al., 2021), and observed GFP-Bqt4 fluorescence intensity in these mutants. Except for the *hul5*Δ mutant, which exhibited a slight increase in the GFP-Bqt4 level, the other mutants showed no detectable changes by fluorescence microscopy (Figure 3-S2). Thus, unidentified E3 ligases appear to function in the INM in cooperation with Doa10 to ubiquitinate Bqt4.

3-4 Bqt4 is an integral membrane protein

Our lab have previously shown that the Bqt4 protein localizes exclusively to the nucleoplasmic side of the INM, and this localization requires its C-terminal helix (Chikashige et al., 2009). However, as this C-terminal helix is predicted to be a weak candidate for the TMD (Figure 3-4A), I examined whether Bqt4 is an integral or a peripheral membrane protein to understand how Bqt4 is removed from the INM before degradation. Therefore, I performed a membrane protein extraction experiment. In brief, cells were lysed, treated under various conditions, and then separated into pellet and supernatant fractions by ultracentrifugation, followed by Western blotting; a protein was expected to enter the pellet fraction if it remained in the lumen or associate with the membrane after the treatment. As a control for a luminal and an integral membrane protein, I used GFP-ADEL (Rossanese et al., 2001) and GFP-Bqt3 (Chikashige et al., 2009), respectively. As shown in Figure 3-4B, all these proteins were extracted from the membrane by treatment with Triton X-100 and 0.5 M NaCl. However, similar to Bqt3, Bqt4 was not dissociated from the membrane by sodium carbonate (pH 11), urea, or NaCl treatments, which can strip peripheral membrane proteins. In contrast, GFP-ADEL was completely released from the membrane by sodium carbonate treatment, as expected for luminal proteins. Thus, Bqt4 is likely to behave as a tail-anchored protein and its C-terminal sequence can act as a TMD that is integrally embedded in the INM.

3-5 Degradation of Bqt4 requires the Cdc48 retrotranslocation complex

The ATPase Cdc48 has been shown to facilitate the degradation of ubiquitinated ERAD membrane substrates by extracting them from the ER membrane in *S. cerevisiae* (Ye et al., 2001; Jarosch et al., 2002; Rabinovich et al., 2002; Wolf and Stolz, 2012). Therefore, I investigated whether Cdc48 is necessary for Bqt4 degradation. To this end, I generated a

cdc48 mutant bearing mutations in both the D1 (P267L) and D2 (A550T) ATPase domains, based on the temperature-sensitive *cdc48-6* allele in *S. cerevisiae* (Schuberth and Buchberger, 2005; Ruggiano et al., 2016) (Figure 3-5A). The *cdc48* mutant (*cdc48-P267L/A550T*) exhibited cold-sensitive growth defects (Figure 3-5B), suggesting that these mutations impaired Cdc48 activity in *S. pombe*. While degradation of Bqt4 is not significantly affected in the Cdc48 mutant *cdc48-P267L/A550T* at the permissive temperature (Figure 3-5C, D), its inactivation of by shifting to the nonpermissive temperature of 16°C elevated the level of GFP-Bqt4 in $bqt3^{+}$ and *bqt3Δ* cells (Figure 3-5E, F). As the ATPase activity of Cdc48 is required for extracting membrane proteins, our results suggest that Bqt4 is extracted from the INM by the Cdc48 complex prior to its degradation.

3-6 The C-terminal TMD of Bqt4 acts as a degradation signal

Our previous work showed that Bqt4 degradation depends on its C-terminal TMD (residues 414-432) (Chikashige et al., 2009). To identify the minimal region of Bqt4 that is sufficient for its degradation, I performed an analysis of truncated C-terminal fragments based on the structure of Bqt4 predicted by AlphaFold2 (Figure 3-6A). The Bqt4 fragment ($Bqt4C^{369-432}$) containing the helix domain and the adjacent intrinsically disordered sequence reproduced behaviors of full-length Bqt4, as shown in Figure 3-1A, that is, localization and responses to BZ, both in the presence and absence of Bqt3 (Figure 3-6B). The helix domain alone ($Bqt4C^{394-432}$) showed weaker localization at the NE and somewhat diffused to the membrane compartments in the cytoplasm; nevertheless, this fragment was degraded in the absence of Bqt3, and its levels increased with BZ treatment (Figure 3-6B). The TMD alone ($Bqt4C^{414-432}$) showed even weaker localization at the NE with diffusion to the cytoplasm, but showed the same responses, that is, degradation in the absence of Bqt3, and increased levels upon BZ treatment (Figure 3-6B). These results indicate that the C-terminal fragment containing

residues 369–432, which might contain an NLS, is sufficient for the localization of Bqt4 to the NE. These results also indicated that the C-terminal TMD of Bqt4 is sufficient for its proteasome-mediated degradation.

To further narrow the TMD of Bqt4 for proteasome-dependent degradation and Bqt3-dependent protection against degradation, I generated constructs with a shorter TMD truncated of the last seven residues (Bqt4C$^{369\text{-}425}$ and Bqt4C$^{414\text{-}425}$). The fragments Bqt4C$^{369\text{-}425}$ and Bqt4C$^{414\text{-}425}$ lost their dependency on Bqt3 for degradation and showed similar behaviors in the presence or absence of Bqt3. While Bqt4C$^{369\text{-}425}$ retained slight localization at the NE and Bqt4C$^{414\text{-}425}$ showed diffuse localization in the cytoplasm, both fragments showed increased signal levels in the presence of BZ. These fragments, lacking the last seven residues, are also substrates of proteasomal degradation in a Bqt3-independent manner (Figure 3-6B). These results suggest that the fragment of residues 414–425 is sufficient for proteasomal degradation and that the fragment of residues 426–432 is required for Bqt3-dependent protection against proteasomal degradation.

3-7 Excess Bqt4 causes deformation of the NE

I observed that inhibition of proteasomal degradation caused striking NE expansion and deformation with irregular protrusions and invaginations, especially in *bqt3*$^{+}$ cells, in which Bqt4 levels were excessively high (Figure 3-1A, C). I hypothesized that the high levels of Bqt4 in these cells were responsible for this abnormal NE morphology. To test this possibility, I inhibited proteasomal degradation in the presence or absence of endogenous Bqt4 and visualized the NE using Ish1-GFP as an NE marker, and then nuclear deformation was assessed by roundness of the nucleus. Only when Bqt4 was present was strong deformation of NE observed upon proteasomal inhibition (see *bqt4*$^{+}$+BZ; Figure 3-7A), suggesting that Bqt4 was an essential factor causing this phenomenon. To ascertain whether

this abnormal phenotype was caused by an accumulation of Bqt4, I overexpressed GFP-Bqt4 under the *nmt1* promoter using YAM2 to control the expression level. YAM2, a chemical compound, suppresses *nmt1* promoter activity depending on its concentration (Nakamura et al., 2011). Overexpression of GFP-Bqt4 at levels similar to proteasomal inhibition reproduced the observed nuclear-deformed morphology, and maximal overexpression of GFP-Bqt4 resulted in even more striking NE proliferation and deformation in both *bqt3*$^{+}$ and *bqt3Δ* cells, indicating that abnormal NE morphology depended on the amount of Bqt4 (Figure 3-7B). Taken together, these results support our hypothesis that Bqt4 is the only protein whose accumulation upon degradation inhibition induces aberrant nuclear morphology. Finally, I investigated whether excess GFP-Bqt4 was toxic. I found that overproduction of GFP-Bqt4 caused a growth defect in both *bqt3*$^{+}$ and *bqt3Δ* strains compared to cells expressing endogenous levels of Bqt4 (Figure 3-7C). Altogether, these observations suggest that Bqt4 plays an important role in regulating NE morphology and that a nuclear proteasomal degradation pathway controlling the quantity of Bqt4 is crucial for nuclear membrane homeostasis.

Chapter 4 Discussion

In this study, I identified the molecular factors required for the degradation of the INM integral protein Bqt4 in *S. pombe* (Figure 4-1). Bqt4 undergoes degradation by an INMAD mechanism involving the Doa10 E3 ligase, which possibly recognizes the C-terminal TMD of Bqt4 as a degron. Subsequently, the AAA-ATPase Cdc48 removes Bqt4 from the INM, and Bqt4 is finally degraded via the nuclear proteasome. I also demonstrated that undegraded Bqt4 accumulating in the INM caused strong deformation of the NE and resulted in growth defects. Bqt4 escapes degradation when interacting with Bqt3 through its C-terminal TMD. Excess amounts of Bqt4 that are unbound to Bqt3 are subjected to INMAD-mediated degradation to avoid the accumulation of Bqt4 at the NE. These findings contribute to our understanding of the significance of INM protein degradation in INM homeostasis.

4-1 Bqt4 is a native INM degradation substrate containing an intramembrane degron

Studies in mammalian cells have suggested that integral INM proteins are largely stable (Toyama et al., 2013; Buchwalter et al., 2019) and it has been difficult to study their turnover. In the budding yeast *S. cerevisiae*, most of the INMAD substrates characterized thus far are not native INM proteins, but rather nuclear soluble proteins (Swanson et al., 2001; Ravid et al., 2006) and ER membrane proteins that are unassembled or mislocalized to the INM (Foresti et al., 2014; Khmelinskii et al., 2014; Natarajan et al., 2020). Thus, our study of Bqt4 provides an opportunity for a native INM substrate to obtain further insight into the mechanisms governing INM protein degradation. Along with several previous studies that reported a handful of native INM substrates (Boban et al., 2014; Pantazopoulou et al., 2016; Smoyer et al., 2019; Koch et al., 2019), our results on the degradation of the INM protein

Bqt4 demonstrate that INMAD is responsible for not only maintaining INM identity by removing foreign proteins but also for maintaining the proteostasis of INM integral components.

An important question is whether INMAD machinery specifically recognizes its substrates. Although a degradation signal has yet to be identified for integral INM substrates of INM-localized E3 ubiquitin ligases, such as Doa10 and the Asi complex, I identified that Bqt4 has an intramembrane degron. This suggests that INMAD may not simply detect and degrade misfolded or mislocalized proteins at the INM, but instead specifically recognizes a substrate to regulate its protein levels.

4-2 An INM protein degradation pathway in *S. pombe*

In *S. cerevisiae*, the Doa10 E3 ubiquitin ligase cooperates with the Asi complex in INMAD (Koch and Yu, 2019; Smoyer and Jaspersen, 2019; Mannino and Lusk, 2022). As homologs of Asi proteins are absent in *S. pombe* as in other species, INMAD mechanisms may be diverse among organisms. However, increasing evidence has shown that the degradation of INM proteins in plants and mammals also employs the UPS and Cdc48/p97 (Tsai et al., 2016; Huang et al., 2020; Krshnan et al., 2022), raising a general mechanism for INM protein degradation.

In *S. cerevisiae*, Doa10 E3 ligase can passively diffuse from the ER to the INM and functions in both ERAD and INMAD (Deng and Hochstrasser, 2006). In particular, Doa10 has been implicated in mediating the degradation of the INM protein Asi2, which itself is a component of INMAD (Boban et al., 2014). In *S. pombe*, Bqt4 degradation also depends on Doa10, indicating that Bqt4 is subject to regulation by INMAD. In addition, our data indicate that *S. pombe* might possess additional unidentified redundant E3 ligases cooperating with Doa10 at the INM. Because Bqt4 is supposed to be recognized by these E3 ligases at its

transmembrane degron, it is expected that the unidentified E3 ligases also localize to the INM ("X(E3)" in Figure 4-1). Similar situations, in which unidentified E3 ligases degrade an INM substrate, have been reported in *S. cerevisiae* (Pantazopoulou et al. 2016). Likewise, INM-localized E3 ligases have yet to be identified in higher eukaryotes. I speculate that the uncharacterized E3 ligases functioning at the INM in *S. pombe* might operate with E2 ubiquitin-conjugating enzymes other than Ubc6 and Ubc7 because degradation of Bqt4 exhibits limited dependence on these enzymes. Thus, it would be of great interest to identify and characterize other E3 ligases and E2 conjugating enzymes that mediate protein degradation at the INM.

The Cdc48 complex plays a central role in the ERAD degradation of ER integral membrane proteins by exerting a pulling force on the ubiquitinated membrane protein via its ATPase activity (Braun, 2002; Rabinovich et al., 2002; Wolf and Stolz, 2012; Bodnar and Rapoport, 2017). Cdc48 has also been implicated in the degradation of the INM proteins Asi1 and Msp3 in *S. cerevisiae* (Pantazopoulou et al. 2016; Koch et al., 2019). In *S. pombe*, Cdc48 mutations at its ATPase active center impair Bqt4 degradation, indicating that ERAD/INMAD degradation also utilizes the Cdc48 complex to extract membrane-embedded substrates and deliver them to the proteasome for proteolysis. Thus, our study demonstrated the presence of a conserved INMAD system in *S. pombe*.

4-3 The biological significance of Bqt4 degradation

The INM protein Bqt4 has been suggested to have non-telomeric functions that are currently unknown, yet vital for cell growth, as double deletion of Bqt4 and Lem2 results in synthetic lethality (Tange et al., 2016; Hirano et al., 2018; Kinugasa et al., 2019). In cells lacking both Bqt4 and Lem2, nuclear envelope rupture occurs in association with the leakage of nuclear proteins into the cytoplasm, suggesting that Bqt4, in cooperation with Lem2, plays essential

roles in maintaining nuclear membrane integrity (Kinugasa et al., 2019). The nuclear membrane rupture phenotype can be rescued by an increased expression of Elo2, a fatty acid elongase that catalyzes the synthesis of very-long-chain fatty acids (Kinugasa et al., 2019). In addition, depletion of Bqt4 and Lem2 also leads to a reduction in the quantity of t20:0/24:0 phytoceramide, the most abundant ceramide species in *S. pombe*, and this reduction can be prevented by the overexpression of Elo2 (Kinugasa et al., 2019). These findings strongly suggest that Bqt4 is involved in nuclear membrane lipid metabolism. Thus, I propose that abnormal accumulation of Bqt4 at the INM may result in excessive lipid synthesis, ultimately leading to nuclear membrane expansion and deformation. One possibility is that Bqt4 promotes the synthesis of phospholipids, a major component of the nuclear membrane. Several lines of evidence suggest that increased phospholipid synthesis from phosphatidic acid induces striking NE membrane deformation (Santos-Rosa et al., 2005; Barbosa et al., 2015). The exact mechanisms leading to the deformed nuclear morphology upon the accumulation of Bqt4 remain to be elucidated. Further investigations will advance our understanding of the role of INM protein degradation in the maintenance of nuclear membrane homeostasis.

Tables and Figures

Table 1. *S. pombe* strains used in this study

Strain	Genotype	Source	Figure
TL204	*h⁻ bqt4Δ::hph lys1⁺::bqt4p-GFP-bqt4*	This study	3-1A-F, 3-2B,C, 3-3A-D, 3-5B, 3-6C-F, 3-8C
TL205	*h⁻ bqt4Δ::hph lys1⁺::bqt4p-GFP-bqt4 bqt3Δ::NAT*	This study	3-1A-F, 3-2B,C, 3-3A-D, 3-4, 3-5B, 3-6C-F, 3-8C
TL288	*h⁻ bqt4Δ::hph lys1⁺::bqt4p-GFP-bqt4 mts3-1*	This study	3-1C, D
TL289	*h⁻ bqt4Δ::hph bqt3Δ::NAT lys1⁺::bqt4p-GFP-bqt4 mts3-1*	This study	3-1C, D
H1N95	*h⁻ bqt4Δ::hph lys1⁺::bqt4p-GFP*	This study	3-1E
TL233	*h⁻ bqt4Δ::hph bqt3Δ::NAT lys1⁺::bqt4p-GFP-bqt4 isp6Δ::bsd*	This study	3-1F
TL234	*h⁻ bqt4Δ::hph bqt3Δ::NAT lys1⁺::bqt4p-GFP-bqt4 atg1Δ:: kan^r*	This study	3-1F
TL290	*h⁻ bqt4Δ::hph lys1⁺::bqt4p-GFP-bqt4 cut8-563*	This study	3-2B, C
TL291	*h⁻ bqt4Δ::hph bqt3Δ::NAT lys1⁺::bqt4p-GFP-bqt4 cut8-563*	This study	3-2B, C
TL215	*h⁻ bqt4Δ::hph bqt3Δ::NAT lys1⁺::bqt4p-GFP-bqt4 doa10Δ::bsd*	This study	3-3A, B, 3-4
TL219	*h⁻ bqt4Δ::hph bqt3Δ::NAT lys1⁺::bqt4p-GFP-bqt4 hrd1Δ:: kan^r*	This study	3-3A, B, 3-4

TL236	*h⁻ bqt4Δ::hph bqt3Δ::NAT lys1⁺::bqt4p-GFP-bqt4 doa10Δ::bsd hrd1Δ:: kan^r*	This study	3-3A, B
TL220	*h⁻ bqt4Δ::hph bqt3Δ::NAT lys1⁺::bqt4p-GFP-bqt4 ubc7Δ:: kan^r*	This study	3-3C, D
TL221	*h⁻ bqt4Δ::hph bqt3Δ::NAT lys1⁺::bqt4p-GFP-bqt4 ubc6Δ:: kan^r*	This study	3-3C, D
TL266	*h⁻ bqt4Δ::hph bqt3Δ::NAT lys1⁺::bqt4p-GFP-bqt4 ubc6Δ:: kan^r ubc7Δ::bsd*	This study	3-3C, D
TL222	*h⁻ bqt4Δ::hph bqt3Δ::NAT lys1⁺::bqt4p-GFP-bqt4 meu34Δ:: kan^r*	This study	3-4
TL224	*h⁻ bqt4Δ::hph bqt3Δ::NAT lys1⁺::bqt4p-GFP-bqt4 san1Δ:: kan^r*	This study	3-4
TL225	*h⁻ bqt4Δ::hph bqt3Δ::NAT lys1⁺::bqt4p-GFP-bqt4 ubr1Δ:: kan^r*	This study	3-4
TL226	*h⁻ bqt4Δ::hph bqt3Δ::NAT lys1⁺::bqt4p-GFP-bqt4 ubr11Δ:: kan^r*	This study	3-4
TL227	*h⁻ bqt4Δ::hph bqt3Δ::NAT lys1⁺::bqt4p-GFP-bqt4 hul5Δ:: kan^r*	This study	3-4
TL267	*h⁻ bqt4Δ::hph bqt3Δ::NAT lys1⁺::bqt4p-GFP-bqt4 dsc1Δ:: kan^r*	This study	3-4
TL292	*h⁻ bqt4Δ::hph bqt3Δ::NAT lys1⁺::bqt4p-GFP-bqt4 cut9-665*	This study	3-4
TL294	*h⁻ bqt4Δ::hph bqt3Δ::NAT lys1⁺::bqt4p-GFP-bqt4 ptr1-1*	This study	3-4

HA1382-3D	*h⁻ lys1-131 ura4-D18 leu1-32 bqt3Δ::LEU2 aur1ʳ::bqt3p-GFP-bqt3*	This study	3-5B
H1N789	*h⁻ lys1+::nmt41p-SS-GFP-ADEL*	This study	3-5B
h-972	*h⁻*	Laboratory stock	3-6B, 3-8C
TL311	*h⁻ lys1-131 cdc48Δ:: kanʳ aur1ʳ::cdc48p-cdc48-P267L/A550T*	This study	3-6B
TL306	*h⁻ bqt4Δ::hph lys1⁺::bqt4p-GFP-bqt4 cdc48Δ:: kanʳ aur1ʳ::cdc48p-cdc48-P267L/A550T*	This study	3-6C-F
TL307	*h⁻ bqt4Δ::hph lys1⁺::bqt4p-GFP-bqt4 bqt3Δ::NAT cdc48Δ:: kanʳ aur1ʳ::cdc48p-cdc48-P267L/A550T*	This study	3-6C-F
TL242	*h⁻ bqt4Δ::hph lys1⁺::bqt4p-GFP-bqt4C$^{369-432}$*	This study	3-7B
TL243	*h⁻ bqt4Δ::hph bqt3Δ::NAT lys1⁺::bqt4p-GFP-bqt4C$^{369-432}$*	This study	3-7B
TL246	*h⁻ bqt4Δ::hph lys1⁺::bqt4p-GFP-bqt4C$^{394-432}$*	This study	3-7B
TL247	*h⁻ bqt4Δ::hph bqt3Δ::NAT lys1⁺::bqt4p-GFP-bqt4C$^{394-432}$*	This study	3-7B
TL248	*h⁻ bqt4Δ::hph lys1⁺::bqt4p-GFP-bqt4C$^{414-432}$*	This study	3-7B
TL249	*h⁻ bqt4Δ::hph bqt3Δ::NAT lys1⁺::bqt4p-GFP-bqt4C$^{414-432}$*	This study	3-7B
TL250	*h⁻ bqt4Δ::hph lys1⁺::bqt4p-GFP-bqt4C$^{369-425}$*	This study	3-7B
TL251	*h⁻ bqt4Δ::hph bqt3Δ::NAT lys1⁺::bqt4p-GFP-bqt4C$^{369-425}$*	This study	3-7B
TL252	*h⁻ bqt4Δ::hph lys1⁺::bqt4p-GFP-bqt4C$^{414-425}$*	This study	3-7B

TL253	*h⁻ bqt4Δ::hph bqt3Δ::NAT lys1⁺::bqt4p-GFP-bqt4C$^{414-425}$*	This study	3-7B
H1N429	*h⁻ lys1⁺::ish1-GFP*	This study	3-8A
H1N546	*h⁺ bqt4Δ::hph lys1⁺::ish1-GFP*	This study	3-8A
TL206	*h⁻ bqt4Δ::hph lys1⁺::nmt1p-GFP-bqt4*	This study	3-8B, C
TL207	*h⁻ bqt4Δ::hph lys1⁺::nmt1p-GFP-bqt4 bqt3Δ::NAT*	This study	3-8B, C

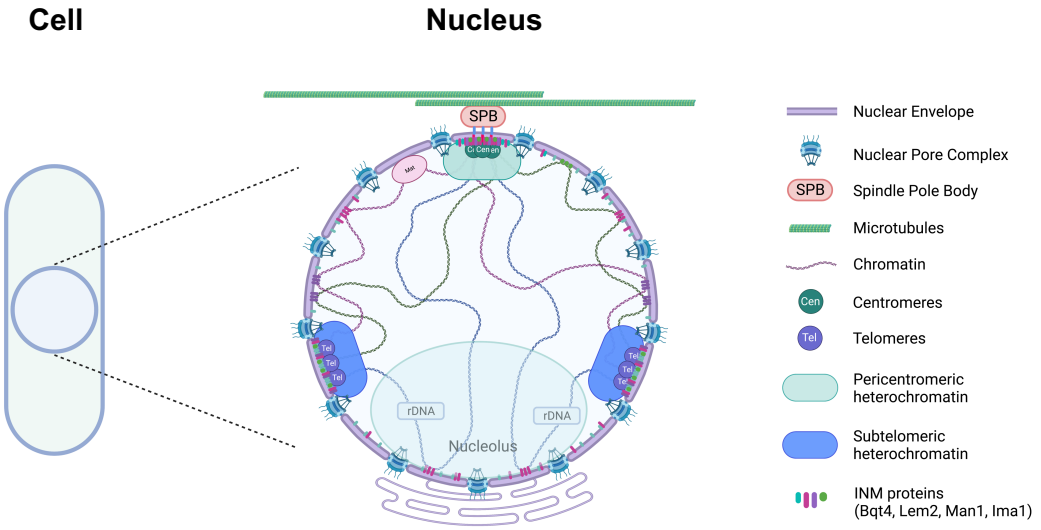

Figure 1-1. The structure of the fission yeast nucleus. Schematic representation of a *S. pombe* cell (left). Magnification of the nucleus, highlighting the spatial organization of the chromosomes (right). This figure was created with Biorender.com.

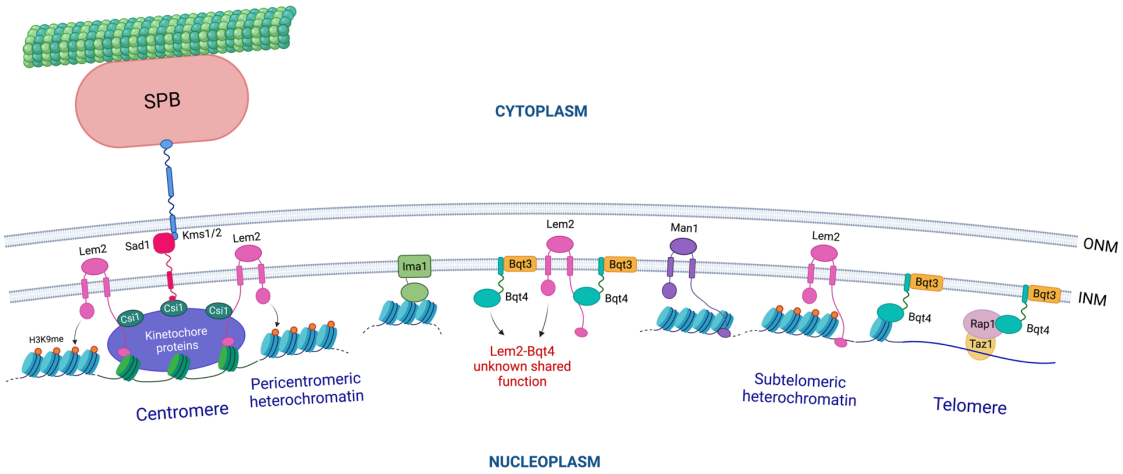

Figure 1-2. The INM proteins in *S. pombe*. The INM proteins (Sad1, Ima1, Lem2, Man1, and Bqt4) interact with various regions of the chromosome, including the centromere and telomere, tethering them to the NE. Some of these proteins (Ima1, Lem2, and Man1) also play pivotal roles in the formation of heterochratin regions beneath the NE. In addition, Lem2 and Bqt4 appear to have unknown functions important for nuclear membrane homeostasis, which is vital to the cell. This figure was created with Biorender.com.

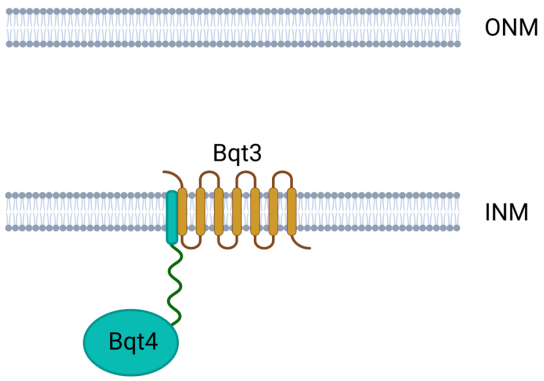

Figure 1-3. Bqt4 interacts with Bqt3 at the INM. Bqt4 protein is predicted to be composed of a structurally defined N-terminal domain, a long linker of less defined structure, and a putative C-terminal TMD, which is required for membrane localization and interaction with Bqt3. Bqt3 is predicted to be a multi-pass transmembrane protein composed of 7 TMDs along its entire length. This figure was created with Biorender.com.

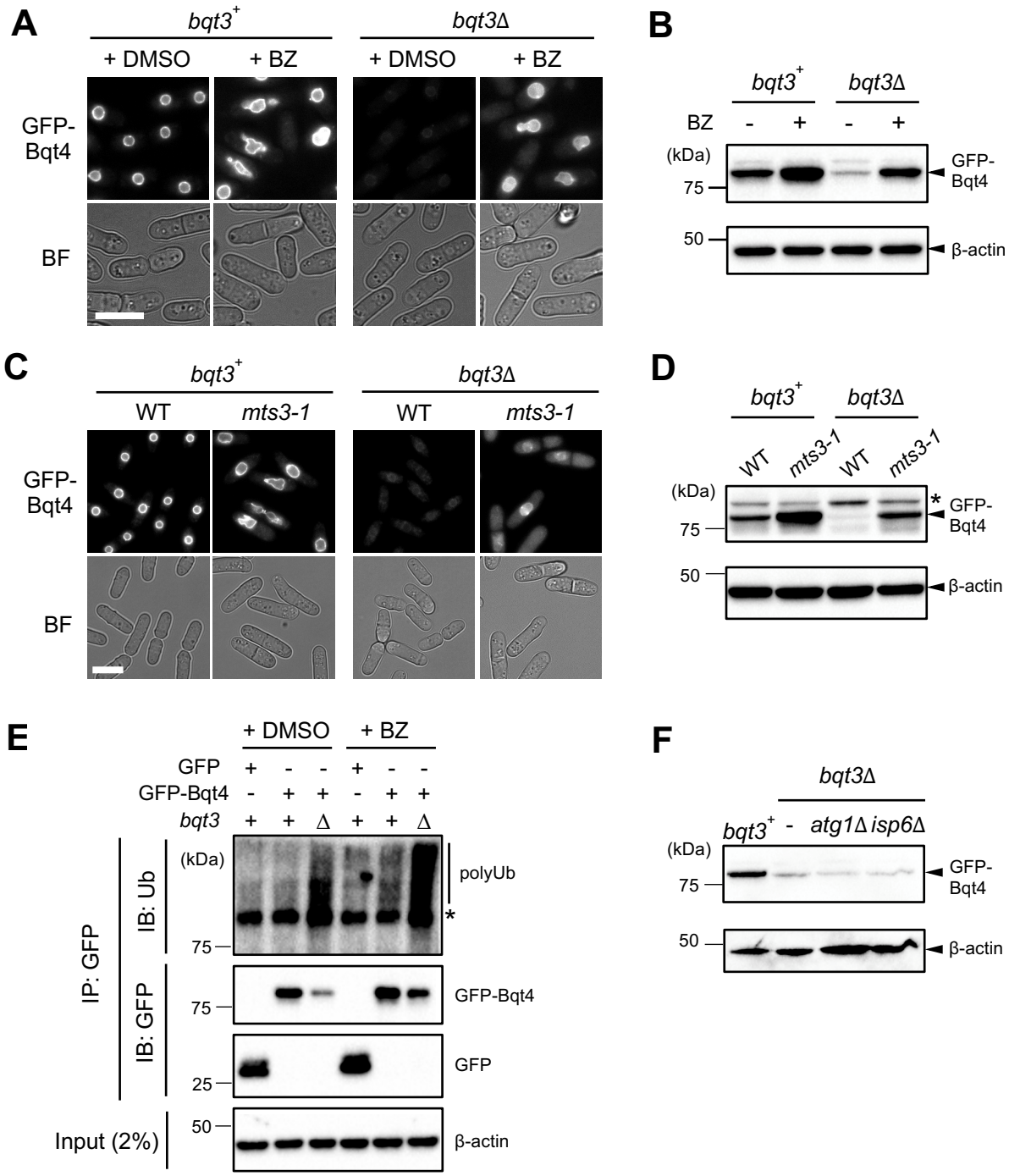

Figure 3-1. Bqt4 protein is degraded by the ubiquitin-proteasome system

(A, B) Cells expressing GFP-Bqt4 in the *bqt3*$^{+}$ or *bqt3*Δ background were treated with vehicle (+DMSO) or the proteasome inhibitor bortezomib (+BZ) for 4 h and subjected to microscopic observation (A) or Western blotting (B). (A) Fluorescence microscopic images of GFP-Bqt4 (upper panels); bright-field images (lower panels). Bar, 10 μm. (B) Protein

amounts of GFP-Bqt4 and β-actin were detected by anti-GFP and anti-β-actin antibodies, respectively. Molecular weight markers are shown on the left.

(C, D) Cells harboring *mts3-1* in the *bqt3*$^{+}$ or *bqt3*Δ background were cultured at a nonpermissive temperature (36°C) for 4 h and subjected to microscopic observation (C) or Western blotting (D). (C) Fluorescence microscopic images of GFP-Bqt4 (upper panels); bright-field images (lower panels). Bar, 10 μm. (D) Protein amounts of GFP-Bqt4 and β-actin were detected as in (B). The asterisk in (D) indicates non-specific bands.

(E) Polyubiqutination of Bqt4 protein. Cells expressing GFP or GFP-Bqt4 in the *bqt3*$^{+}$ or *bqt3*Δ background were treated with vehicle (+DMSO) or the proteasome inhibitor bortezomib (+BZ) for 4 h. After denaturing the proteins, GFP and GFP-Bqt4 were immunoprecipitated with anti-GFP antibody (IP). The precipitated proteins were detected by anti-ubiquitin or anti-GFP antibodies, respectively (IB). β-actin was used as a loading control. Molecular weight markers are shown on the left.

(F) No Bqt4 degradation by the lysosome-autophagy system. Deletion of *atg1* (*atg1*Δ) or *isp6* (*isp6*Δ) was introduced into the *bqt3*Δ cells. Protein amounts of GFP-Bqt4 and β-actin in these cells were detected as in (B). Molecular weight markers are shown on the left.

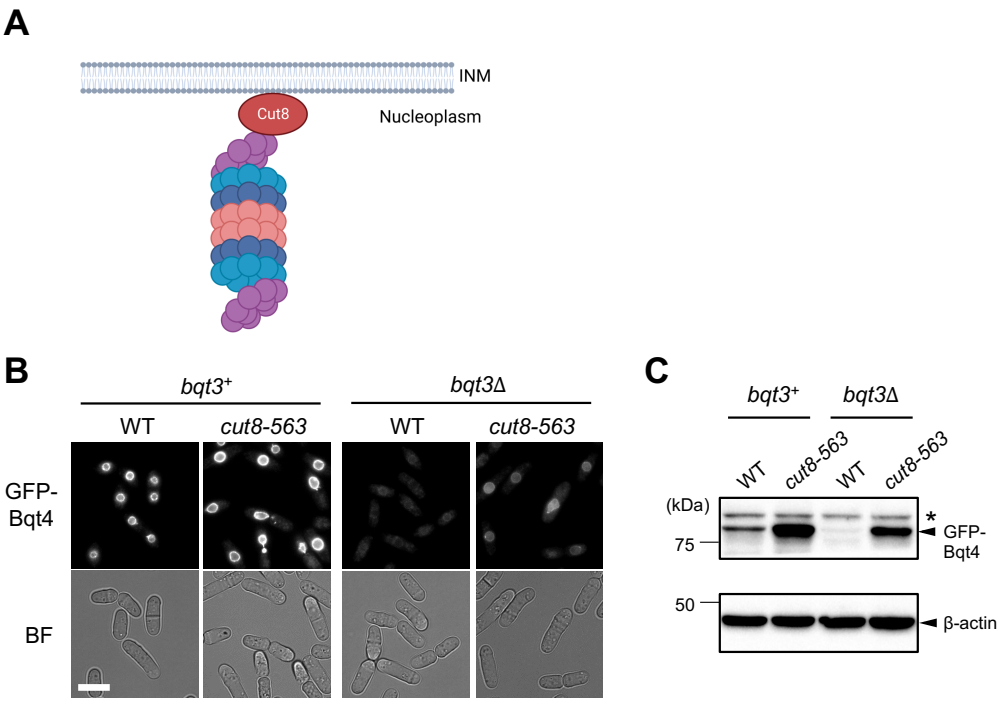

Figure 3-2. Bqt4 degradation occurs in the nucleus

(A) A model of Cut8 tethering the proteasome to the nuclear membrane, which enriches the proteasomes in the nucleus (Tatebe and Yanagida, 2000; Takeda and Yanagida, 2005). (B, C) Cells harboring *cut8-655 ts* mutation in the *bqt3*$^{+}$ or *bqt3*Δ background were cultured at a nonpermissive temperature (36°C) for 4 h and subjected to microscopic observation (B) or Western blotting (C). (B) Fluorescence images of GFP-Bqt4 (upper panels); bright-field images (lower panels). Bar, 10 μm. (C) Protein levels of GFP-Bqt4 and β-actin were detected using anti-GFP and anti-β-actin antibodies, respectively. The asterisk indicates non-specific bands. Molecular weight markers are shown on the left.

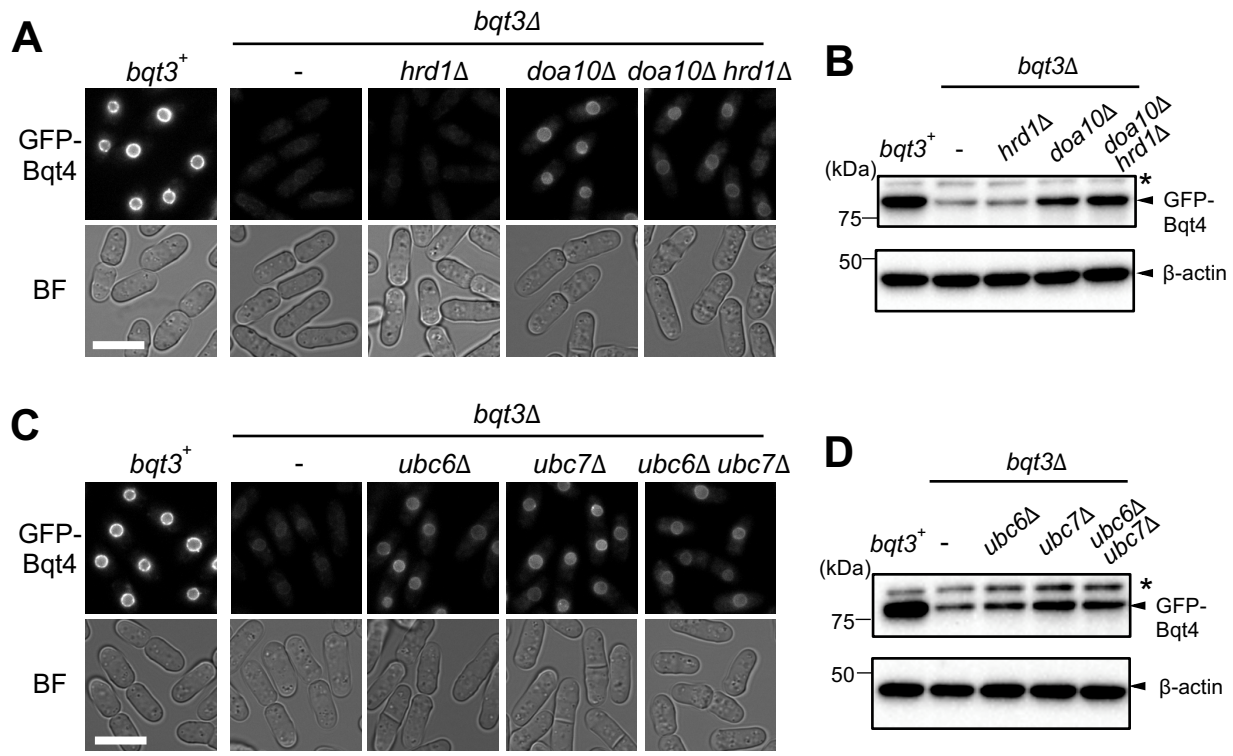

Figure 3-3. Bqt4 is a substrate of the Doa10 complex

Bqt4 protein levels in *doa10, ubc6* and *ubc7* mutants. (A, B) Cells harboring *hrd1* (*hrd1*Δ), *doa10* (*doa10*Δ) single deletion, or *hrd1* and *doa10* double deletion (*hrd1*Δ *doa10*Δ) in *bqt3*Δ background were cultured at 30°C for 16 h, and then subjected to microscopic observation (A) or Western blotting (B). (A) Fluorescence microscopic images of GFP-Bqt4 (upper panels); bright-field images (lower panels). Bar, 10 μm. (B) Protein levels of GFP-Bqt4 and β-actin were detected using anti-GFP and anti-β-actin antibodies, respectively. (C, D) Cells harboring *ubc6* (*ubc6*Δ), *ubc7* (*ubc7*Δ) single deletion, or *ubc6* and *ubc7* double deletion (*ubc6*Δ *ubc7*Δ) in *bqt3*Δ background were cultured at 30°C for 16 h, and then subjected to microscopic observation (C) or Western blotting (D). (C) Fluorescence microscopic images of GFP-Bqt4 (upper panels); bright-field images (lower panels). Bar, 10 μm. (D) Protein levels of GFP-Bqt4 and β-actin were detected using anti-GFP and anti-β-actin antibodies, respectively. The asterisk indicates non-specific bands. Molecular weight markers are shown on the left.

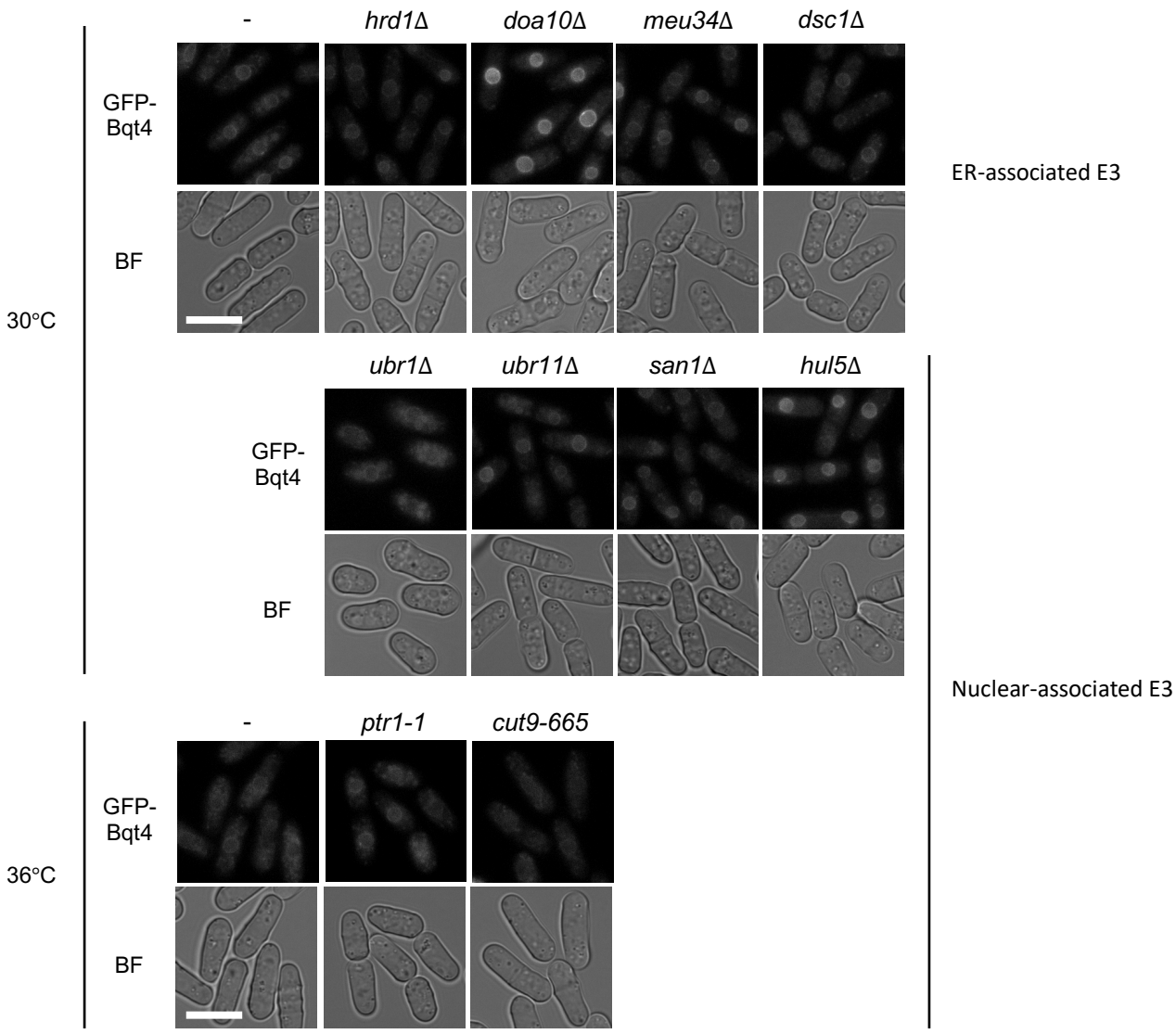

Figure 3-4. Most nuclear- or ER-associated E3 ligases have a minimal role in Bqt4 degradation

Fluorescence images of GFP-Bqt4 in mutants are shown. Deletion or mutation of E3 ligases localized in the ER (*meu34*Δ, *dsc1*Δ) or functioning in the nucleus (*san1*Δ, *ubr1*Δ, *ubr11*Δ, *hul5*Δ, *ptr1-1*, *cut9-665*) was introduced in *bqt3*Δ cells expressing GFP-Bqt4. The cells were cultured at 30°C for 16 h or shifted to 36°C for 4 h for *ts* mutants and then observed using fluorescence microscopy. Bars: 10 μm.

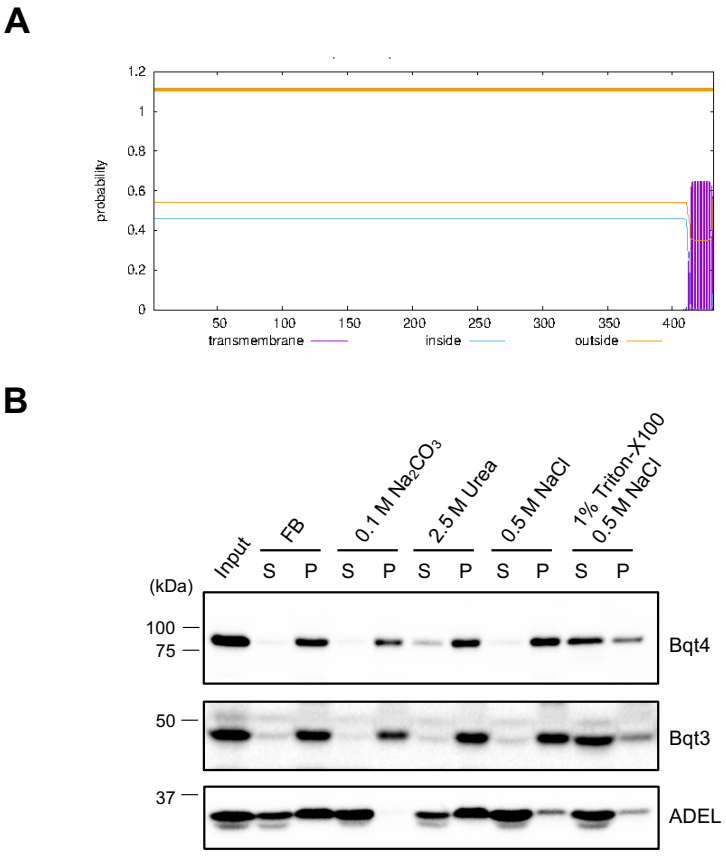

Figure 3-5. Bqt4 is an integral membrane protein

(A) The transmembrane helices of Bqt4 were predicted by the TMHMM-2.0 prediction server (https://services.healthtech.dtu.dk/service.php?TMHMM-2.0). The vertical and horizontal axes indicate the prediction probability and amino acid residues of Bqt4, respectively.

(B) Cells expressing GFP-Bqt4, GFP-Bqt3, or GFP-ADEL were mixed at a 1:1:1 ratio and lysed by bead beating. After removing cell debris, the extracts were treated under various conditions, as shown on the top. The extracts were fractionated by ultracentrifugation into supernatant (S) and pellet (P), and then GFP-tagged proteins in each fraction were detected by Western blotting. Molecular weight markers are shown on the left.

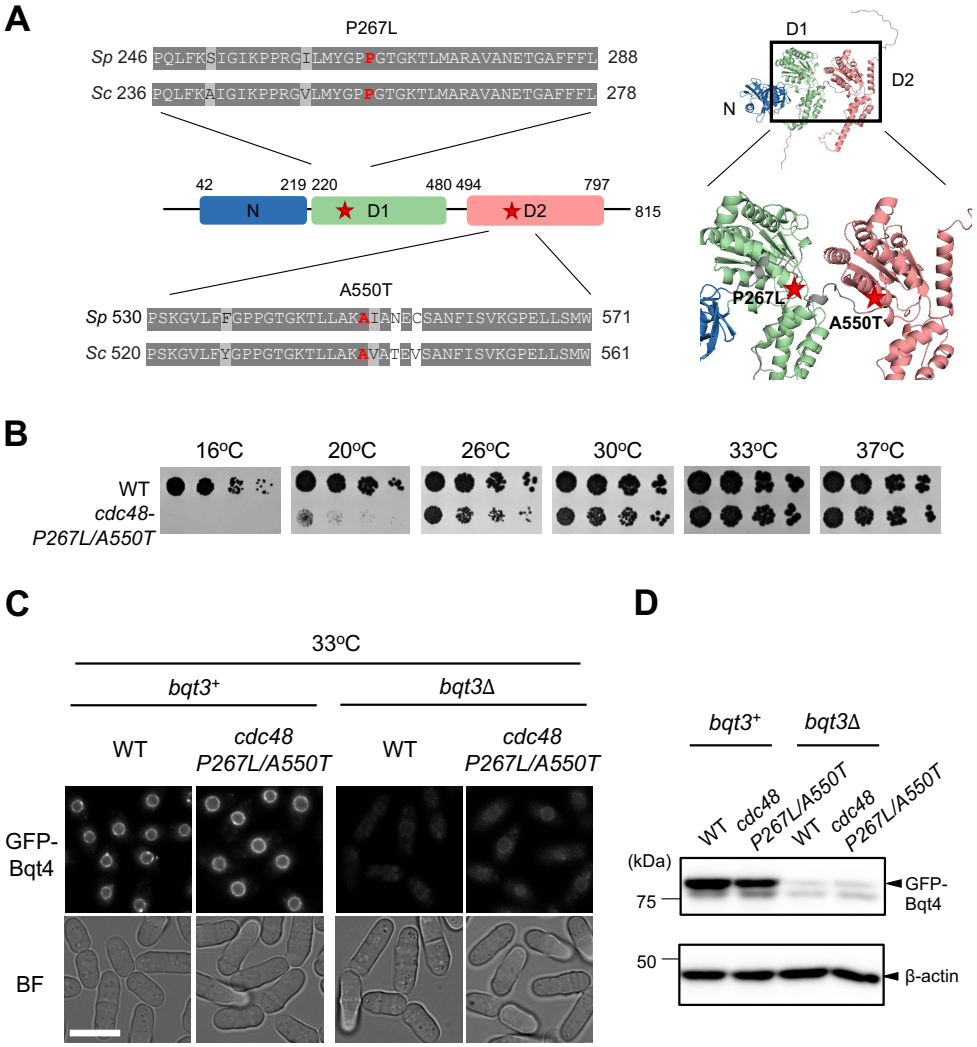

Figure 3-6. Removal of Bqt4 requires the Cdc48 retrotranslocation complex

(A) The Cdc48 mutant used in this study. Left panel: the amino acid sequence alignment around the D1 and D2 domains of *S. pombe* (*Sp*) and *S. cerevisiae* (*Sc*) Cdc48. Gray and light gray shades denote identical and similar amino acids, respectively (top and bottom). The amino acids indicated by red (P267 and A550; correspond to red stars in the schematic diagram in the middle) are both mutated in this study (P267L/A550T). Right panel: the mutation sites are shown in the predicted three-dimensional structure of Cdc48 by AlphaFold2 (https://alphafold.ebi.ac.uk/entry/Q9P3A7).

(B) Temperature sensitivity of *cdc48-P267L/A550T* mutant. Five-fold serially diluted cells harboring *cdc48-P267L/A550T* mutant were spotted on the YES plate, and cultured at different temperatures as indicated at the bottom.

(C, D) Cells harboring the cdc48-P267L/A550T mutant in the *bqt3*$^{+}$ or *bqt3Δ* background were cultured at 33°C for 15 h and subjected to microscopic observation (C) or Western blotting (D). (C) Fluorescence microscopic images of GFP-Bqt4 (upper panels); bright-field images (lower panels). Bar: 10 μm. (D) Protein amounts of GFP-Bqt4 and β-actin were detected by anti-GFP and anti-β-actin antibodies, respectively. Molecular weight markers are shown on the left.

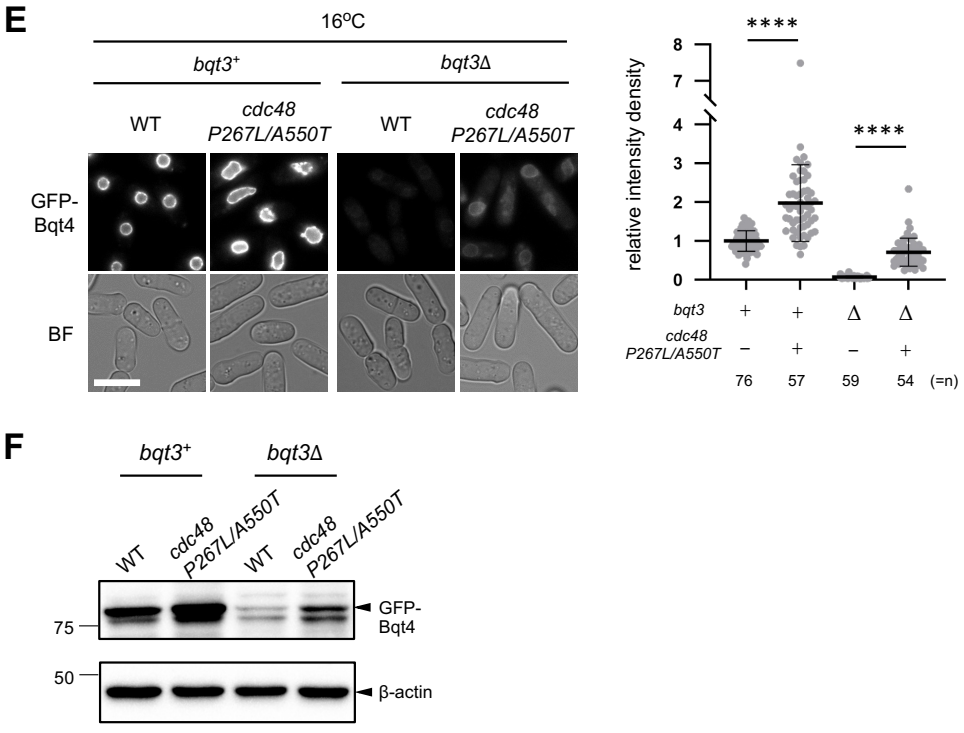

Figure 3-6 (continued). (E, F) Effect of hypomorphic mutation of *cdc48* on Bqt4 degradation. Cells harboring the *cdc48-P267L/A550T* mutant in the *bqt3*$^{+}$ or *bqt3*Δ background were cultured at a nonpermissive temperature (16°C) for 15 h and subjected to microscopic observation (E) or Western blotting (F). (E) Left panels: Fluorescence microscopic images of GFP-Bqt4 (upper panels); bright-field images (lower panels). Bar: 10

μm. Right panel: the fluorescence intensities in the nuclei were quantified and the relative values were plotted. The mean values are plotted with standard deviation on the right panel. The number of the cells analyzed is shown at the bottom. $****p < 0.0001$ via two-tailed unpaired student's *t*-test. (F) Protein amounts of GFP-Bqt4 and β-actin were detected by anti-GFP and anti-β-actin antibodies, respectively. Molecular weight markers are shown on the left.

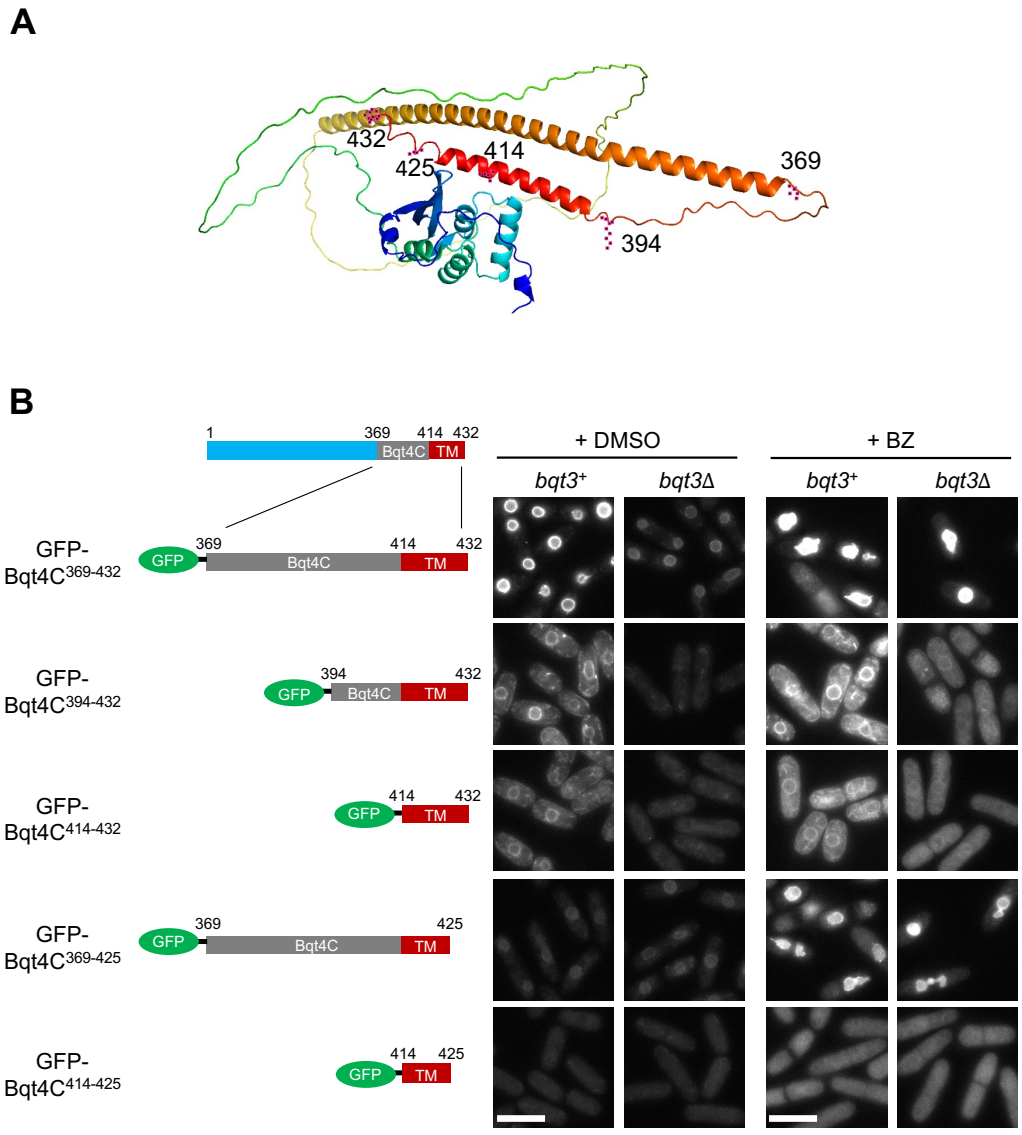

Figure 3-7. The C-terminal sequence of Bqt4 is a degron

(A) The three-dimensional structure of Bqt4 predicted by AlphaFold2 was obtained from the website (https://alphafold.ebi.ac.uk/entry/O60158).

(B) The C-terminal fragments of Bqt4 are shown as a cartoon on the left. These fragments were expressed as GFP-fused proteins in the *bqt3*$^{+}$ or *bqt3*Δ cells. The cells were treated with vehicle (+DMSO) or the proteasome inhibitor bortezomib (+BZ) for 4 h and then observed by fluorescence microscopy. Bars: 10 μm.

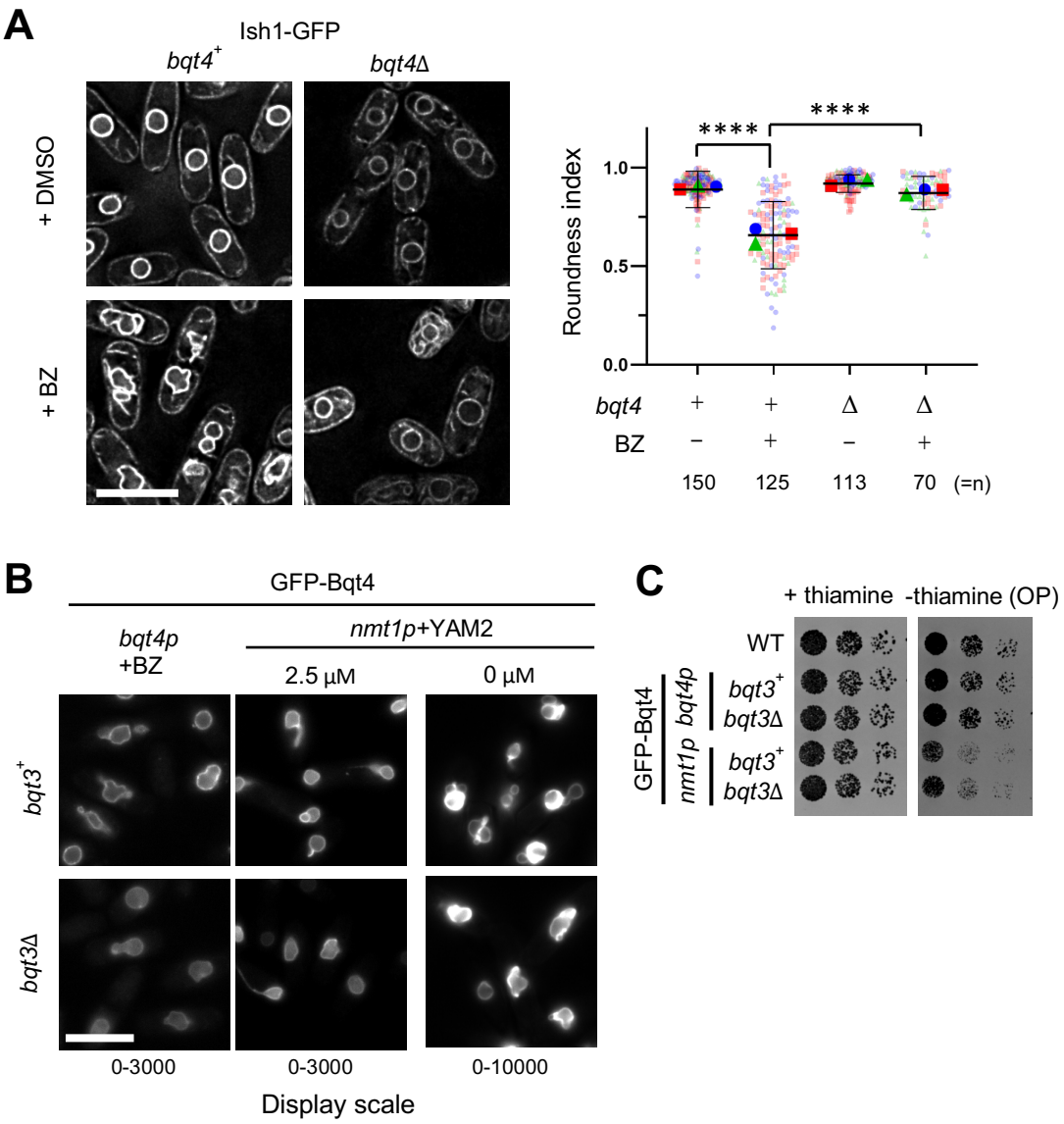

Figure 3-8. Excess Bqt4 causes nuclear envelope deformation

(A) Left panels: Fluorescence microscopic images of Ish1-GFP in *bqt4*$^{+}$ or *bqt4*Δ cells. Ish1-GFP was used as a nuclear membrane marker (Asakawa et al., 2022). The cells were treated with vehicle (+DMSO) or the proteasome inhibitor bortezomib (+BZ) for 4 h. The images were deconvoluted using the SoftWoRx software (v7.0.0). Bar: 10 μm. Right panel: The roundness index of the nucleus in these cells was measured from three independent experiments (shown in blue, green, and red, respectively) and plotted as a superplot (Lord et al., 2020) (right panel). The roundness index one indicates a perfect circle. The solid blue circle, green triangle, and red square represent the mean value of the measurements in each

experiment, respectively. Black horizontal lines represent the mean value for all data that is shown with standard deviation. *n* at the bottom right represents the total number of cells analyzed. $****p < 0.0001$ via two-tailed unpaired student's *t*-test.

(B) Fluorescence microscopic images of GFP-Bqt4 in the *bqt3*$^{+}$ or *bqt3*Δ cells. GFP-Bqt4 was overproduced under the *nmt1* promoter in the presence or absence of 2.5 μM YAM2 in EMMG for 20 and 18 h, respectively. For comparison, *bqt4p*-GFP-Bqt4 fluorescence images of cells treated with BZ (*bqt4p*+BZ) are reproduced in Figure 3-1A with different display scales. Bar: 10 μm.

(C) Growth defects by Bqt4 overproduction. GFP-Bqt4 was overproduced under *bqt4* (*bqt4p*) or *nmt1* promoter (*nmt1p*) in the *bqt3*$^{+}$ or *bqt3*Δ cells. Five-fold serially diluted cells were spotted on the EMMG plate in the presence or absence of thiamine for 4 days. WT indicates wildtype.

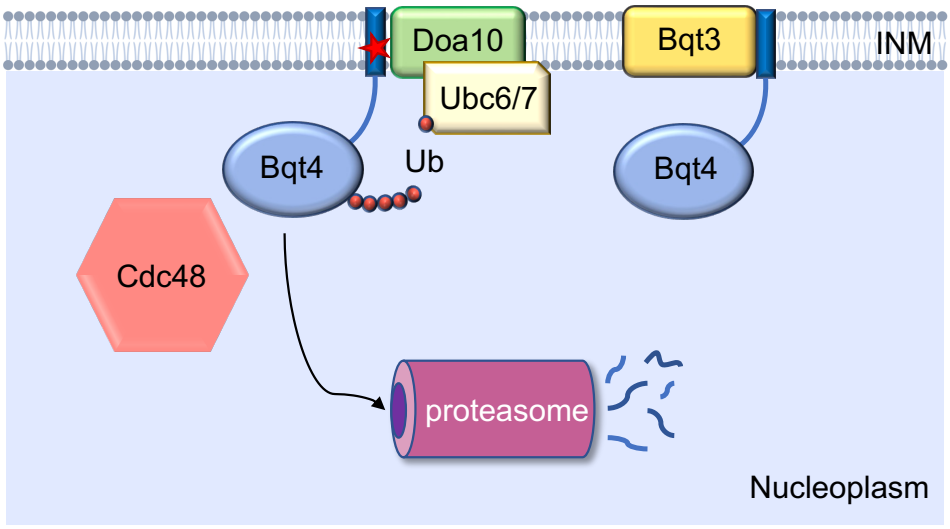

Figure 4-1. A model of INM protein degradation of Bqt4

Excess Bqt4, with exposed TMD as a degradation signal, is recognized and ubiquitinated by INM-associated E3 ubiquitin ligase complexes, including Doa10 and additional unidentified E3 ligases. Ubiquitinated Bqt4 is then actively dislocated from the INM by the AAA-ATPase Cdc48 complex and transferred to the nuclear proteasome for proteolysis.

References

Asakawa, H., Hirano, Y., Shindo, T., Haraguchi, T., Hiraoka, Y., 2022. Fission yeast Ish1 and Les1 interact with each other in the lumen of the nuclear envelope. Genes Cells 27, 643–656. https://doi.org/10.1111/gtc.12981

Barbosa, A.D., Sembongi, H., Su, W.-M., Abreu, S., Reggiori, F., Carman, G.M., Siniossoglou, S., 2015. Lipid partitioning at the nuclear envelope controls membrane biogenesis. Mol. Biol. Cell 26, 3641–3657. https://doi.org/10.1091/mbc.E15-03-0173

Boban, M., Pantazopoulou, M., Schick, A., Ljungdahl, P.O., Foisner, R., 2014. A nuclear ubiquitin-proteasomal pathway targets inner nuclear membrane protein Asi2 for degradation. J. Cell Sci. jcs.153163. https://doi.org/10.1242/jcs.153163

Buchwalter, A., Schulte, R., Tsai, H., Capitanio, J., Hetzer, M., 2019. Selective clearance of the inner nuclear membrane protein emerin by vesicular transport during ER stress. eLife 8, e49796. https://doi.org/10.7554/eLife.49796

Chen, C.-Y., Chi, Y.-H., Mutalif, R.A., Starost, M.F., Myers, T.G., Anderson, S.A., Stewart, C.L., Jeang, K.-T., 2012. Accumulation of the Inner Nuclear Envelope Protein Sun1 Is Pathogenic in Progeric and Dystrophic Laminopathies. Cell 149, 565–577. https://doi.org/10.1016/j.cell.2012.01.059

Chikashige, Y., Tsutsumi, C., Yamane, M., Okamasa, K., Haraguchi, T., Hiraoka, Y., 2006. Meiotic Proteins Bqt1 and Bqt2 Tether Telomeres to Form the Bouquet Arrangement of Chromosomes. Cell 125, 59–69. https://doi.org/10.1016/j.cell.2006.01.048

Chikashige, Y., Yamane, M., Okamasa, K., Tsutsumi, C., Kojidani, T., Sato, M., Haraguchi, T., Hiraoka, Y., 2009. Membrane proteins Bqt3 and -4 anchor telomeres to the nuclear envelope to ensure chromosomal bouquet formation. J. Cell Biol. 187, 413–427. https://doi.org/10.1083/jcb.200902122

Christianson, J.C., Carvalho, P., 2022. Order through destruction: how ER-associated protein degradation contributes to organelle homeostasis. EMBO J. 41. https://doi.org/10.15252/embj.2021109845

Ciechanover, A., 2005. Intracellular protein degradation: from a vague idea thru the lysosome and the ubiquitin–proteasome system and onto human diseases and drug targeting. Cell Death Differ. 12, 1178–1190. https://doi.org/10.1038/sj.cdd.4401692

Deng, M., Hochstrasser, M., 2006. Spatially regulated ubiquitin ligation by an ER/nuclear membrane ligase. Nature 443, 827–831. https://doi.org/10.1038/nature05170

Deshaies, R.J., Joazeiro, C.A.P., 2009. RING Domain E3 Ubiquitin Ligases. Annu. Rev. Biochem. 78, 399–434. https://doi.org/10.1146/annurev.biochem.78.101807.093809

Ebrahimi, H., Masuda, H., Jain, D., Cooper, J.P., 2018. Distinct 'safe zones' at the nuclear envelope ensure robust replication of heterochromatic chromosome regions. eLife 7, e32911. https://doi.org/10.7554/eLife.32911

Enam, C., Geffen, Y., Ravid, T., Gardner, R.G., 2018. Protein Quality Control Degradation in the Nucleus. Annu. Rev. Biochem. 87, 725–749. https://doi.org/10.1146/annurev-biochem-062917-012730

Finley, D., 2009. Recognition and Processing of Ubiquitin-Protein Conjugates by the Proteasome. Annu. Rev. Biochem. 78, 477–513. https://doi.org/10.1146/annurev.biochem.78.081507.101607

Foresti, O., Rodriguez-Vaello, V., Funaya, C., Carvalho, P., 2014. Quality control of inner nuclear membrane proteins by the Asi complex. Science 346, 751–755. https://doi.org/10.1126/science.1255638

Franić, D., Zubčić, K., Boban, M., 2021. Nuclear Ubiquitin-Proteasome Pathways in Proteostasis Maintenance. Biomolecules 11, 54. https://doi.org/10.3390/biom11010054

Gonzalez, Y., Saito, A., Sazer, S., 2012. Fission yeast Lem2 and Man1 perform fundamental functions of the animal cell nuclear lamina. Nucleus 3, 60–76. https://doi.org/10.4161/nucl.18824

Gordon, C., McGurk, G., Wallace, M., Hastie, N.D., 1996. A Conditional Lethal Mutant in the Fission Yeast 26 S Protease Subunit mts3+ Is Defective in Metaphase to Anaphase Transition. J. Biol. Chem. 271, 5704–5711. https://doi.org/10.1074/jbc.271.10.5704

Groettrup, M., Pelzer, C., Schmidtke, G., Hofmann, K., 2008. Activating the ubiquitin family: UBA6 challenges the field. Trends Biochem. Sci. 33, 230–237. https://doi.org/10.1016/j.tibs.2008.01.005

Habeck, G., Ebner, F.A., Shimada-Kreft, H., Kreft, S.G., 2015. The yeast ERAD-C ubiquitin ligase Doa10 recognizes an intramembrane degron. J. Cell Biol. 209, 261–273. https://doi.org/10.1083/jcb.201408088

Hershko, A., Ciechanover, A., 1998. THE UBIQUITIN SYSTEM. Annu. Rev. Biochem. 67, 425–479. https://doi.org/10.1146/annurev.biochem.67.1.425

Hirano, Y., Asakawa, H., Sakuno, T., Haraguchi, T., Hiraoka, Y., 2020. Nuclear Envelope Proteins Modulating the Heterochromatin Formation and Functions in Fission Yeast. Cells 9, 1908. https://doi.org/10.3390/cells9081908

Hirano, Y., Kinugasa, Y., Asakawa, H., Chikashige, Y., Obuse, C., Haraguchi, T., Hiraoka, Y., 2018. Lem2 is retained at the nuclear envelope through its interaction with Bqt4 in fission yeast. Genes Cells 23, 122–135. https://doi.org/10.1111/gtc.12557

Hiraoka, Y., Maekawa, H., Asakawa, H., Chikashige, Y., Kojidani, T., Osakada, H., Matsuda, A., Haraguchi, T., 2011. Inner nuclear membrane protein Ima1 is dispensable for intranuclear positioning of centromeres: S. pombe inner nuclear

membrane proteins. Genes Cells 16, 1000–1011. https://doi.org/10.1111/j.1365-2443.2011.01544.x

Hochstrasser, M., 1996. UBIQUITIN-DEPENDENT PROTEIN DEGRADATION. Annu. Rev. Genet. 30, 405–439. https://doi.org/10.1146/annurev.genet.30.1.405

Hu, C., Inoue, H., Sun, W., Takeshita, Y., Huang, Y., Xu, Y., Kanoh, J., Chen, Y., 2019. The Inner Nuclear Membrane Protein Bqt4 in Fission Yeast Contains a DNA-Binding Domain Essential for Telomere Association with the Nuclear Envelope. Structure 27, 335-343.e3. https://doi.org/10.1016/j.str.2018.10.010

Huang, A., Tang, Y., Shi, X., Jia, M., Zhu, J., Yan, X., Chen, H., Gu, Y., 2020. Proximity labeling proteomics reveals critical regulators for inner nuclear membrane protein degradation in plants. Nat. Commun. 11, 3284. https://doi.org/10.1038/s41467-020-16744-1

Janin, A., Bauer, D., Ratti, F., Millat, G., Méjat, A., 2017. Nuclear envelopathies: a complex LINC between nuclear envelope and pathology. Orphanet J. Rare Dis. 12, 147. https://doi.org/10.1186/s13023-017-0698-x

Jarosch, E., Taxis, C., Volkwein, C., Bordallo, J., Finley, D., Wolf, D.H., Sommer, T., 2002. Protein dislocation from the ER requires polyubiquitination and the AAA-ATPase Cdc48. Nat. Cell Biol. 4, 134–139. https://doi.org/10.1038/ncb746

Katta, S.S., Smoyer, C.J., Jaspersen, S.L., 2014. Destination: inner nuclear membrane. Trends Cell Biol. 24, 221–229. https://doi.org/10.1016/j.tcb.2013.10.006

Khmelinskii, A., Blaszczak, E., Pantazopoulou, M., Fischer, B., Omnus, D.J., Le Dez, G., Brossard, A., Gunnarsson, A., Barry, J.D., Meurer, M., Kirrmaier, D., Boone, C., Huber, W., Rabut, G., Ljungdahl, P.O., Knop, M., 2014. Protein quality control at the inner nuclear membrane. Nature 516, 410–413. https://doi.org/10.1038/nature14096

Kinuagsa, Y., Hirano, Y., Sawai, M., Ohno, Y., Shindo, T., Asakawa, H., Chikashige, Y., Shibata, S., Kihara, A., Haraguchi, T., Hiraoka, Y., 2019. Very-long-chain fatty acid elongase Elo2 rescues lethal defects associated with loss of the nuclear barrier function. J. Cell Sci. jcs.229021. https://doi.org/10.1242/jcs.229021

Koch, B., Yu, H.-G., 2019. Regulation of inner nuclear membrane associated protein degradation. Nucleus 10, 169–180. https://doi.org/10.1080/19491034.2019.1644593

Koch, B.A., Jin, H., Tomko, R.J., Yu, H.-G., 2019. The anaphase-promoting complex regulates the degradation of the inner nuclear membrane protein Mps3. J. Cell Biol. 218, 839–854. https://doi.org/10.1083/jcb.201808024

Kohda, T.A., Tanaka, K., Konomi, M., Sato, M., Osumi, M., Yamamoto, M., 2007. Fission yeast autophagy induced by nitrogen starvation generates a nitrogen source that drives adaptation processes. Genes Cells 12, 155–170. https://doi.org/10.1111/j.1365-2443.2007.01041.x

Mannino, P.J., Lusk, C.P., 2022. Quality control mechanisms that protect nuclear envelope identity and function. J. Cell Biol. 221, e202205123. https://doi.org/10.1083/jcb.202205123

Matsuyama, A., Arai, R., Yashiroda, Y., Shirai, A., Kamata, A., Sekido, S., Kobayashi, Y., Hashimoto, A., Hamamoto, M., Hiraoka, Y., Horinouchi, S., Yoshida, M., 2006. ORFeome cloning and global analysis of protein localization in the fission yeast Schizosaccharomyces pombe. Nat. Biotechnol. 24, 841–847. https://doi.org/10.1038/nbt1222

Mekhail, K., Moazed, D., 2010. The nuclear envelope in genome organization, expression and stability. Nat. Rev. Mol. Cell Biol. 11, 317–328. https://doi.org/10.1038/nrm2894

Nakamura, Y., Arai, A., Takebe, Y., Masuda, M., 2011. A chemical compound for controlled expression of nmt1-driven gene in the fission yeast Schizosaccharomyces pombe. Anal. Biochem. 412, 159–164. https://doi.org/10.1016/j.ab.2011.01.039

Nakayama, K.I., Nakayama, K., 2006. Ubiquitin ligases: cell-cycle control and cancer. Nat. Rev. Cancer 6, 369–381. https://doi.org/10.1038/nrc1881

Natarajan, N., Foresti, O., Wendrich, K., Stein, A., Carvalho, P., 2020. Quality Control of Protein Complex Assembly by a Transmembrane Recognition Factor. Mol. Cell 77, 108-119.e9. https://doi.org/10.1016/j.molcel.2019.10.003

Nielsen, S., Poulsen, E., Rebula, C., Hartmann-Petersen, R., 2014. Protein Quality Control in the Nucleus. Biomolecules 4, 646–661. https://doi.org/10.3390/biom4030646

Pantazopoulou, M., Boban, M., Foisner, R., Ljungdahl, P.O., 2016. Cdc48 and Ubx1 participate in an inner nuclear membrane associated degradation pathway that governs the turnover of Asi1. J. Cell Sci. jcs.189332. https://doi.org/10.1242/jcs.189332

Pawar, S., Kutay, U., 2021. The Diverse Cellular Functions of Inner Nuclear Membrane Proteins. Cold Spring Harb. Perspect. Biol. 13, a040477. https://doi.org/10.1101/cshperspect.a040477

Pickart, C.M., Eddins, M.J., 2004. Ubiquitin: structures, functions, mechanisms. Biochim. Biophys. Acta BBA - Mol. Cell Res. 1695, 55–72. https://doi.org/10.1016/j.bbamcr.2004.09.019

Rabinovich, E., Kerem, A., Fröhlich, K.-U., Diamant, N., Bar-Nun, S., 2002. AAA-ATPase p97/Cdc48p, a Cytosolic Chaperone Required for Endoplasmic Reticulum-Associated Protein Degradation. Mol. Cell. Biol. 22, 626–634. https://doi.org/10.1128/MCB.22.2.626-634.2002

Ravid, T., Kreft, S.G., Hochstrasser, M., 2006. Membrane and soluble substrates of the Doa10 ubiquitin ligase are degraded by distinct pathways. EMBO J. 25, 533–543. https://doi.org/10.1038/sj.emboj.7600946

Rossanese, O.W., Reinke, C.A., Bevis, B.J., Hammond, A.T., Sears, I.B., O'Connor, J., Glick, B.S., 2001. A Role for Actin, Cdc1p, and Myo2p in the Inheritance of Late Golgi Elements in Saccharomyces cerevisiae. J. Cell Biol. 153, 47–62. https://doi.org/10.1083/jcb.153.1.47

Rotin, D., Kumar, S., 2009. Physiological functions of the HECT family of ubiquitin ligases. Nat. Rev. Mol. Cell Biol. 10, 398–409. https://doi.org/10.1038/nrm2690

Ruggiano, A., Foresti, O., Carvalho, P., 2014. ER-associated degradation: Protein quality control and beyond. J. Cell Biol. 204, 869–879. https://doi.org/10.1083/jcb.201312042

Ruggiano, A., Mora, G., Buxó, L., Carvalho, P., 2016. Spatial control of lipid droplet proteins by the ERAD ubiquitin ligase Doa10. EMBO J. 35, 1644–1655. https://doi.org/10.15252/embj.201593106

Santos-Rosa, H., Leung, J., Grimsey, N., Peak-Chew, S., Siniossoglou, S., 2005. The yeast lipin Smp2 couples phospholipid biosynthesis to nuclear membrane growth. EMBO J. 24, 1931–1941. https://doi.org/10.1038/sj.emboj.7600672

Schuberth, C., Buchberger, A., 2005. Membrane-bound Ubx2 recruits Cdc48 to ubiquitin ligases and their substrates to ensure efficient ER-associated protein degradation. Nat. Cell Biol. 7, 999–1006. https://doi.org/10.1038/ncb1299

Smoyer, C.J., Jaspersen, S.L., 2019. Patrolling the nucleus: inner nuclear membrane-associated degradation. Curr. Genet. 65, 1099–1106. https://doi.org/10.1007/s00294-019-00971-1

Smoyer, C.J., Smith, S.E., Gardner, J.M., McCroskey, S., Unruh, J.R., Jaspersen, S.L., 2019. Distribution of Proteins at the Inner Nuclear Membrane Is Regulated by the Asi1 E3 Ligase in *Saccharomyces cerevisiae*. Genetics 211, 1269–1282. https://doi.org/10.1534/genetics.119.301911

Steglich, B., Filion, G., van Steensel, B., Ekwall, K., 2012. The inner nuclear membrane proteins Man1 and Ima1 link to two different types of chromatin at the nuclear periphery in *S. pombe*. Nucleus 3, 77–87. https://doi.org/10.4161/nucl.18825

Stewart, M.D., Ritterhoff, T., Klevit, R.E., Brzovic, P.S., 2016. E2 enzymes: more than just middle men. Cell Res. 26, 423–440. https://doi.org/10.1038/cr.2016.35

Swanson, R., Locher, M., Hochstrasser, M., n.d. A conserved ubiquitin ligase of the nuclear envelope/endoplasmic reticulum that functions in both ER-associated and Mat␣2 repressor degradation 16.

Takeda, K., Mori, A., Yanagida, M., 2011. Identification of Genes Affecting the Toxicity of Anti-Cancer Drug Bortezomib by Genome-Wide Screening in S. pombe. PLoS ONE 6, e22021. https://doi.org/10.1371/journal.pone.0022021

Takeda, K., Yanagida, M., 2005. Regulation of Nuclear Proteasome by Rhp6/Ubc2 through Ubiquitination and Destruction of the Sensor and Anchor Cut8. Cell 122, 393–405. https://doi.org/10.1016/j.cell.2005.05.023

Tange, Y., Chikashige, Y., Takahata, S., Kawakami, K., Higashi, M., Mori, C., Kojidani, T., Hirano, Y., Asakawa, H., Murakami, Y., Haraguchi, T., Hiraoka, Y., 2016. Inner nuclear membrane protein Lem2 augments heterochromatin formation in response to nutritional conditions. Genes Cells 21, 812–832. https://doi.org/10.1111/gtc.12385

Tatebe, H., Yanagida, M., 2000. Cut8, essential for anaphase, controls localization of 26S proteasome, facilitating destruction of cyclin and Cut2. Curr. Biol. 10, 1329–1338. https://doi.org/10.1016/S0960-9822(00)00773-9

Toyama, B.H., Savas, J.N., Park, S.K., Harris, M.S., Ingolia, N.T., Yates, J.R., Hetzer, M.W., 2013. Identification of Long-Lived Proteins Reveals Exceptional Stability of Essential Cellular Structures. Cell 154, 971–982. https://doi.org/10.1016/j.cell.2013.07.037

Tsai, P.-L., Zhao, C., Turner, E., Schlieker, C., 2016. The Lamin B receptor is essential for cholesterol synthesis and perturbed by disease-causing mutations. eLife 5, e16011. https://doi.org/10.7554/eLife.16011

Varshavsky, A., 2012. The Ubiquitin System, an Immense Realm. Annu. Rev. Biochem. 81, 167–176. https://doi.org/10.1146/annurev-biochem-051910-094049

Vembar, S.S., Brodsky, J.L., 2008. One step at a time: endoplasmic reticulum-associated degradation. Nat. Rev. Mol. Cell Biol. 9, 944–957. https://doi.org/10.1038/nrm2546

Wolf, D.H., Stolz, A., 2012. The Cdc48 machine in endoplasmic reticulum associated protein degradation. Biochim. Biophys. Acta BBA - Mol. Cell Res. 1823, 117–124. https://doi.org/10.1016/j.bbamcr.2011.09.002

Wong, X., Stewart, C.L., 2020. The Laminopathies and the Insights They Provide into the Structural and Functional Organization of the Nucleus. Annu. Rev. Genomics Hum. Genet. 21, 263–288. https://doi.org/10.1146/annurev-genom-121219-083616

Ye, Y., Meyer, H.H., Rapoport, T.A., 2001. The AAA ATPase Cdc48/p97 and its partners transport proteins from the ER into the cytosol. Nature 414, 652–656. https://doi.org/10.1038/414652a

Acknowledgements

First and foremost, I would like to express my immense gratitude and respect to my supervisors, Prof. Hiraoka and Prof. Haraguchi, for accepting me into their lab and giving me the opportunity to learn and work on a truly exciting project. Their invaluable insights and expertise have been instrumental in shaping this thesis, and I am truly honored to work under their supervision.

I would also like to express my deep appreciation to Dr. Hirano for being a mentor who has always been there whenever I needed help. I could not have gone so far without his support, advice, and discussion, which have been critical in helping me overcome the challenges during my experiments.

I would also like to extend my sincere thanks to Dr. Asakawa for his valuable contributions and advice, Dr. Sakuno for his discussion and encouragement, and to Ms. Otsuki and Ms. Kubota for their technical assistance.

I am grateful to my committee members, Prof. Fukagawa, Prof. Hirose, Prof. Ikeda, and Prof. Okamoto, for their insightful feedback during the process.

Last but certainly not least, I would like to send my heartfelt thanks to my beloved wife for her unconditional love and unwavering support. I could not have accomplished this work without her by my side.

List of achievements

Publications

Toan Khanh Le, Yasuhiro Hirano, Haruhiko Asakawa, Koji Okamoto, Tokuko Haraguchi and Yasushi Hiraoka. A ubiquitin-proteasome pathway degrades the inner nuclear membrane protein Bqt4 to maintain nuclear membrane homeostasis. bioRxiv doi: 10.1101/2022.12.29.522265. Under review with ***Journal of Cell Science***.

Presentations

Toan Khanh Le, Yasuhiro Hirano, Tokuko Haraguchi, Yasushi Hiraoka. Inner nuclear membrane protein Bqt4 is degraded by a Doa10-dependent proteasomal pathway to prevent nuclear envelope deformation. Oral presentation at the 44th Annual Meeting of the Molecular Biology Society of Japan, Yokohama, Japan, 2021.